



UNIVERSIDAD CARLOS III DE MADRID

GRADO EN INGENIERÍA MECÁNICA

TRABAJO FIN DE GRADO  
MICRO-FAST FOR THE SINTERING OF THE  
SUPERCONDUCTOR MATERIAL YBCO

**Tutors:**

Marco Antonio Álvarez Valenzuela

Ignacio Valiente Blanco

**Author:**

Natalia Sánchez Ruiz

*To my father*

## ACKNOWLEDGEMENTS

*I would like to express my deep and sincere gratitude to my supervisors Mr. Marco Álvarez Valenzuela and Mr. Ignacio Valiente Blanco, for giving me the opportunity to work on this project in collaboration with the University of Strathclyde, under the supervision of Professor Yi Qin. They offered me the support, generous guidance and understanding, which made possible for me to carry out this present work.*

*I would like to thank my fellows, Kunlan Huang, Muhammad-bin-zulkipli, Hasan Hijji and Luis Rubio who has been working with me, sharing their knowledge and guiding me since the first day I arrived to Glasgow until the last one, with the best attitude and predisposition.*

*I am grateful to all my friends from Maravillas, the Amapolas team, my Pilis and Nora for being always there when I needed them and for being a really important part of my life and also to my classmates Silvia Marco, Roberto Molina and Jorge Berlana because without them, my career would have been much harder.*

*I would like to finish with a special gratitude to my father, mother, sisters and brother, brothers in law, nephews and nieces who has given me the love, support, strength and positivism to face every obstacle I found in my life and who have taught me important values, which made me become the person I am today.*

# TABLE OF CONTENT

<b>Abstract and summary</b> .....	<b>1</b>
<b>1. Introduction</b> .....	<b>2</b>
1.1 Yttrium Barium Copper Oxide.....	2
1.1.1 Background.....	3
1.1.2 Structure.....	4
1.1.2.1 Perovskite Structure.....	4
1.1.2.2 Structure of YBCO.....	5
1.1.2.3 Anisotropy of oxygen.....	6
1.1.3 General Consideration of HTS.....	8
1.1.4 Anisotropy and grain connectivity.....	11
1.1.5 Thermal properties.....	13
1.1.6 Mechanical properties.....	14
1.1.7 Applications of HTS.....	16
1.1.7.1 Superconducting Quantum Interference Devices.....	16
1.1.7.2 Josephson junction devices.....	19
1.1.7.3 Electronic applications.....	19
1.2 Process.....	20
1.2.1 Obtaining powders.....	20
1.2.2 Synthesis process.....	21
1.2.3 Sintering process.....	24
1.2.3.1 Sintering theory.....	24
1.2.3.2 General considerations.....	25

1.2.3.3 State-of-the-art of sintering of process of YBCO .....	26
1.2.4 Microforming .....	30
1.2.4.1 Miniature manufacturing .....	30
1.2.4.2 Size effects .....	31
1.2.4.3 Mechanical properties .....	33
1.2.5 Annealing process .....	34
<b>2. Objectives and motivation .....</b>	<b>41</b>
<b>3. Experiment .....</b>	<b>43</b>
3.1 Micro-FAST .....	43
3.1.1 Configuration .....	44
3.1.2 Process .....	45
3.1.3 Experiments .....	49
3.1.4.1 Experiment No. 4-1 .....	49
3.1.4.2 Experiment No. 4-4 .....	50
3.1.4.3 Experiment No. 4-5 .....	52
3.1.4.4 Experiment No. 4-26 .....	53
3.1.4.5 Experiment No. 4-27 .....	55
3.2 Gleeble Machine .....	57
3.2.1 The monitoring and programing .....	57
3.2.2 Mechanical .....	58
3.2.3 General specifications of the mechanical system .....	59

3.2.4 Electrical and thermal properties .....	60
<b>4. Analysis and Result .....</b>	<b>61</b>
4.1Relative density .....	61
4.2 XRD analysis.....	67
4.3 SEM and EDX analysis .....	70
4.3.1 YBCO-Test 1.....	71
4.3.1 YBCO-3.....	72
4.3.1 YBCO-5.....	73
4.3.1 YBCO-6.....	74
<b>5. Conclusions.....</b>	<b>76</b>
<b>6. Problems to be solved.....</b>	<b>78</b>
<b>7. References.....</b>	<b>79</b>

## **Abstract**

In the last twenty years, a large number of investigations and research groups, for the development of miniaturization of products and devices used in the industry, can be found. It has been noticed that the demand for micro-scale manufactured parts has experimented a strong increased. A novel microforming technology, named Micro-FAST has become one of the most promising methods for micromanufacturing with a competitive and efficient low cost, which results a very important requirement to take into account nowadays.

Micro-FAST is the field assisted sintering technique and it was first proposed by a group of researchers for the forming of microcomponents. Some of the researchers, working on the improvement and development of this technique, are part of the Design, Manufacturing and Engineering Management department of the university of Strathclyde, where the experiments mentioned in this project have been carried out. Following the knowledge and previous work they have performed with different materials, in this project it has been realized a Micro-FAST using a superconductor material, Yttrium Barium Copper Oxide, known as YBCO or Y-123.

Oxide superconductors are presenting a high attractive for technical applications recently, since it has been demonstrated they can act as superconductors at liquid nitrogen temperature. Because of this, it has been considered it can be a great challenge to carry out a Micro-FAST with this kind of material, as it is something that is no record on any previous report or magazine.

This project consists in 6 chapters, where can be found a full study of the features of this superconductor material as well as of the characteristics and considerations to take into account for the production of dense YBCO bulk from powders of this material, using Micro-FAST. It also shows the resulting samples obtained after the sintering process carried out in a 3800 Gleeble machine at the Imperial College in London. The different parameters selected for the several experiment are indicated and it can be also observed a deep analysis of the microstructure and the relative density of the samples using high quality devices provided by the university.

The goal of the present work is to fabricate highly dense YBCO body by Micro-FAST in order to improve the sintering time and also analyse the effect on the microstructure and density when some parameters, such as sintering temperature, pressure, heating rate and/or holding time, are changed.

## 1. INTRODUCTION:

### 1.1 Yttrium Barium Copper Oxide.

The enormous amount of electrical current with a perfect and stable current characteristics and high energy losses and also providing unique effects, such as levitation or energy storage, are the main factors that make superconductors very attractive to be studied [1]. These lead to possible economic development as well as the production of new products and services. The applications of High Temperature Ceramic Superconductors, HTCS, can help to save electrical energy as the decrease of the dissipation of the heat and in the total energy production, result great environment and economic benefits.

Yttrium Barium Copper Oxide is considered one of the most promising HTCS known nowadays, which opens many paths to different groups of researchers and investigations of different routes to sinter this material in order to improve its superconductivity features. It results very difficult to underestimate the role HTCS have been played, speaking of materials research progresses through the world, and the main reason for this can be attributed to their potential applications. YBCO shows a single superconducting phase  $\text{YBa}_2\text{Cu}_3\text{O}_x$  with a transition temperature,  $T_c$ , of 90K. In the late 80's it was though superconductivity studies could be only carried out by high equipped laboratories, but it has been demonstrated this is no longer true, due to the increase of the transition temperature as this material present. This  $T_c$  above 77K, at which nitrogen can be found in liquid phase acting as the cooler for this superconductor material, gives the opportunity to analyse superconductivity properties in common laboratories. Nitrogen results to be inexpensive and environmentally friendly compare to other cooler, such as Helium, used for cooling previous superconductors with a lower transition temperature.

It has been also observed that a single YBCO crystal has higher carrying capacity of the electrical current compare to other HCTS crystals. While others ceramics oxide and non-oxide conductors under 5 Tesla magnetic fields, YBCO ceramics can outperform this by a factor of ten or more. However, several technological backwards have been reported for HCTS, which the main ones are they are brittle and that they degrade under common environmental influences. Because of these disadvantages, several worldwide research groups have been working on the conversion of raw HCTS powders into useful materials and products.

### 1.1.1 Background

The superconductivity is a phenomenon first introduced by Herke Kamerlingh-Onnes in 1911 with the discovery of mercury wire with zero electrical resistance at 4.2K, which implied the transmission of current applied at any distance without losses, storage of energy, or large magnetic fields. It was noticed that these materials behaved as normal conductors when the current density was lower than a specific value, this value was called critical current density,  $J_c$ ; or when the magnetic field was under the critical value,  $H_c$  [2].

It was in the 1950s and 1960s when several developments were carried out and it was discovered some materials which could remain superconducting at higher fields and currents. This introduced the fabrication of useful superconducting magnets. These materials are known as superconductors type-II and the name comes because they show two critical magnetic fields,  $H_{c1}$  and  $H_{c2}$ [3], and when the magnetic field applied is in between these values is when they act as superconductors. This will be explained with more details in section 1.1.3.

Another important discovery in order to understand the mechanism of superconductivity was the isotope effect by E. Maxwell and Serin et al. in 1950, independently from each other [4, 5]. This effect explains the dependence of the critical temperature for some superconductors with the isotopic mass, i.e. the mass of a single particle, showing that the lattice vibrations are involved in the superconductivity. The attractive coupling between electrons is through this.

Since the discovery of this phenomenon, many researches have been focus on the study of this in order to obtain superconductor with high transition temperature. Until 1986, the highest temperature observed in a superconductor was 23.2K and it had to be cooled by Helium in liquid state, which results an expensive process and sometimes even unreliable [3]. But in that year, Müller and Bednorz [6, 7] reported the possible superconductivity presented in a ceramic material, La-Ba-Cu-O, with a transition temperature of 30K. Since the confirmation made by the University of Tokyo about this discovery, the era of “High-Temperature Superconductivity” was introduced [8]. Before 1986 finished, it was presented more advances about metal oxides with higher transition temperature, ending at the beginning of 1987 with the discovery of the superconductor material Y-Ba-Cu-O, generally known as YBCO, which shows a  $T_c$  around 90K [9]. This material was superconducting in liquid state nitrogen, which led to less cost as nitrogen is easier to obtain than helium and the system used with it is less complex. This leads to the possibility of realizing investigations at normal laboratory in order to produce YBCO, something unthinkable when the investigations about superconducting first started.

In 1988 different research groups from China, Japan and U.S were found in order to obtain superconductivity in oxides with copper contained without rare earth materials, i.e.

the fifteen lanthanides, as well as scandium and yttrium. With the incorporation of bismuth or thallium a transition temperature of 127K could be reached, which showed several advantages as obtaining  $T_c$  above 77K (operation temperature of nitrogen in liquid state) is advantageous because it has been noticed the increased of the critical current density when  $T/T_c$  decreases. Also, these new materials show more stability than the rare earth superconductive materials, as they do not react with water or lose oxygen [3]. It has been reported nowadays several of these bulk superconductors as electric motors, bearings, flywheel or persistent current switch and there is a great window opened for future research groups with these materials [10].

It has been noticed some difficulties when synthesized by reacting  $Y_2O_3$  and  $BaCO_3$ . It was observed that a long calcination time was required in order to obtain single-phase YBCO when one of the react used was  $BaCO_3$  as the decomposition rate of carbonates is relatively slow [11]. Another problem found with this superconductor synthesized is the carbon retention in the sintered compacts, which forms a solid solution with YBCO and stays permanent in those  $Ba-CO_3$  types in the crystal structure. This effect leads to lower temperature transition and causes an effect in the critical current density.

Several investigation and studies have been made in order to improve these effects, for example using  $BaO_2$  instead of  $BaCO_3$  to avoid the carbon retention but it was observed that the great thermal behaviour of YBCO cuprates were missing [10]. Also, it was demonstrated that micron-size YBCO powder could be fabricated using nitrates precursor. As  $CO_2$  was no evolved during the process, a shorter time was able to be achieved but the preparation of single-phase YBCO superconducting powder was impossible as it required several steps of calcinations with intermittent mixing. It was found that the solid-state was not enough for the homogeneous mixing preparation at the molecular level.

One of the main backwards of the synthesis of YCBO powder using a nitrate precursor was the low content of oxygen found in the calcined powder, which is needed to obtain a great densification, and the generation of  $NO_x$  gases, which is not accepted from an environment point of view [12].

### **1.1.2 Structure:**

#### **1.1.2.1 Perovskite Structure**

There are some solid materials, which show a combination of metallic elements and non-metals, normally oxygen [13]. These materials are ceramics with a Perovskite structure and they show a particular atomic accordance. They can be described by the generalised and ideal formula  $ABX_3$ , where the structure consists in a cube shape with three different chemical elements with a ratio of 1:1:3 for A, B and X. The metallic cations are the one

---

corresponding to A and B, being the X atoms the non-metallic anions. Between the two metallic cations, A is the largest one, which lies in the centre of each cube. B cations are found occupying all the eight corners and the X anions at the mid-points of the twelve edges of the cube. The best way to explain this structure is observing at the image below.

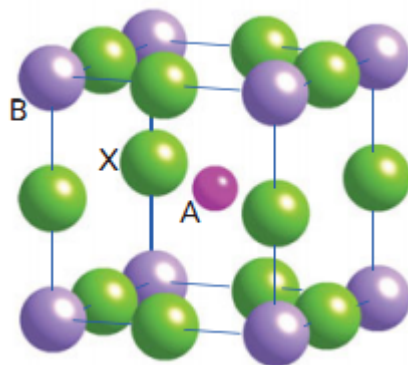


Figure 1. Example of a perovskite structure  $ABX_3$ .

#### 1.1.2.2 The structure of YBCO:

Yttrium Barium Copper Oxide, which general formula of the family is  $YBa_2Cu_3O_{7-x}$ , shows an orthorhombic symmetry, and the compound  $YBa_2Cu_3O_7$  is superconducting at a transition temperature around 90K. In the  $ab$  plane, the structure shows two Cu-O sheets, and along the  $b$ -axis it can be observed Cu-O chains, so it can be said that the structure is a perovskite with an oxygen deficit [14]. An example of a perovskite structure can be found in figure 1. In the case of YBCO, the purple atoms named as B correspond to the metallic cation Cu. Around this element it can be found the six oxygen ions, which are denoted in the image by the letter X (green atoms). The small atom placed in the centre, denoted by A, corresponds with the yttrium. If the oxygen atoms are eliminated from this ideal perovskite lattice, it is obtained  $YBa_2Cu_3O_7$ , which units cell contains A layer of Cu-O where copper (Cu1) is surrounded by four oxygen atoms; a layer of BaO and another one of Cu-O (Cu2), this one surrounded by five oxygen atoms, which form a polyhedron; and a layer of yttrium, short of four oxygen. Based on this description the sequence of the  $ab$  plane can be defined as: Y-CuO-BaO-CuO<sub>2</sub>-BaO-CuO<sub>2</sub>-Y.

The presence of oxygen atoms in the chains found along the  $b$ -axis is crucial for superconductivity. From the general formula mention before,  $YBa_2Cu_3O_{7-x}$ , it is known that the value of  $x$  is observed in a range from 0 to 1 and  $7-x$  corresponds with the oxygen content. Depending on this value, YBCO can show a tetragonal structure or an orthorhombic

structure. These two different structures can be seen in the figure 2. When  $x=1$ , the tetragonal structure  $YBa_2Cu_3O_6$  is achieved, where there are no chain oxygen and Cu in  $b$ -axis is in the  $1+$  state, which correspond to the non-superconducting one. Therefore it can be noticed that the unit cell parameter,  $a$ ,  $b$  and  $c$  vary with the stoichiometry of the oxygen. In the case of  $x=0$ , the structure is completely orthorhombic, figure 2 (b).

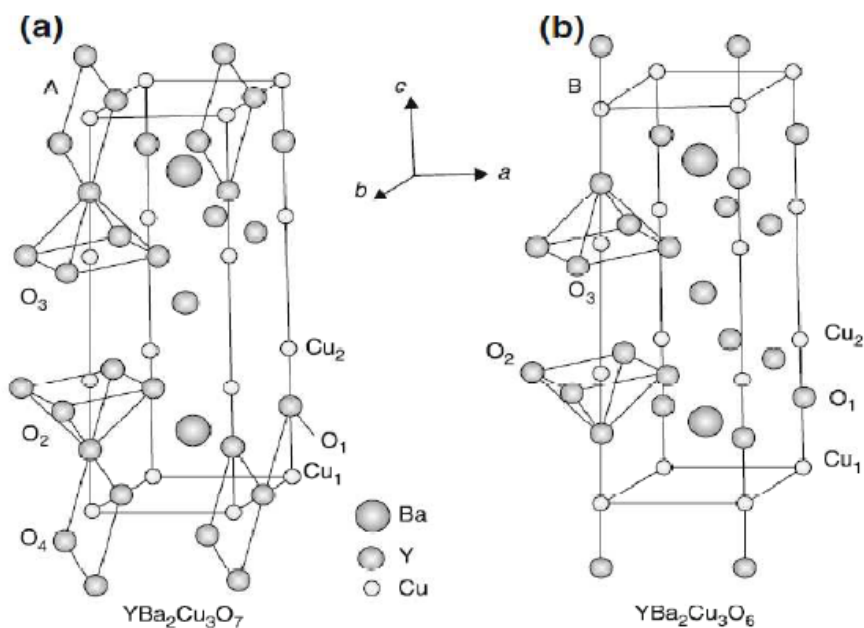


Figure 2. (a) Orthorhombic structure  $YBa_2Cu_3O_7$  and (b) tetragonal structure  $YBa_2Cu_3O_6$ .

Because all the mention above, it can be noticed that bulk properties strongly depend on the manner of synthesis and treatment, due to the effect on crystal size, alignment and density and also due to the type of lattice defects.

### 1.1.2.3 Anisotropy of oxygen

Because the  $YBa_2Cu_3O_{7-x}$  lattice is orthorhombic the diffusion in this compound can be considered anisotropic. The independent diffusion coefficients, which describe this symmetry of the diffusion in a crystal, are parallel to each main crystallographic axis [15]. An extended explanation about the anisotropy and grain connectivity will be carried out in section 1.1.4. Because the structure of the CuO plane varies highly from the other crystal's planes, the anisotropy can be very pronounced. The diffusion in the direction along the  $c$ -axis is generally slower compare to the one in the  $ab$  plane; this is attributed to the oxygen ion vacancies in the structure of  $YBa_2Cu_3O_{7-x}$ .

Following the figure 3, it is explained in several reports that oxygen ions vacancies can be considered equally distributed on the O(1) and O(5) sites, when it presents a high-temperature tetragonal phase. When the temperature is reduced, these vacancies usually tend to be organised on the O(5) sites. The site occupancy and also the stoichiometry depend on the temperature and on the oxygen partial pressure [16]. For the case of the orthorhombic structure, all the sites of O(5) are found unoccupied and the O(1) sites occupied.

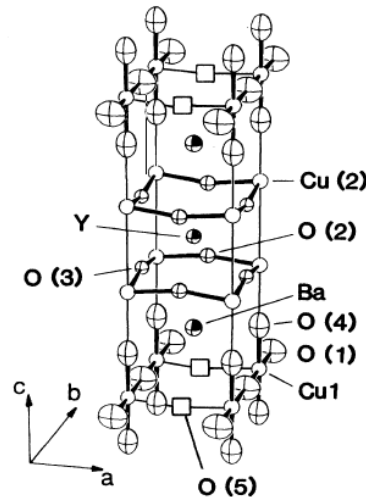


Figure 3. Structure of  $YBa_2Cu_3O_{7-x}$  [16]

The value of  $7-x$ , which means the content of oxygen in the structure, is therefore an important factor that must be taken into account in order to analyse the superconducting properties of the samples. It is needed to control the value of  $x$  to obtain high transition temperature samples. It has been demonstrated in some report papers that in the orthorhombic phase, the parameters  $a$  and  $c$  decrease when the content of oxygen increases, but the  $b$ -parameter increases. The typical range where the value of the  $c$ -axis parameter is found is from  $11.8391 \text{ \AA}$ , for the tetragonal phase; to  $11.660 \text{ \AA}$ , in the case of orthorhombic structure [17].

Many experimental methods have been carried out nowadays in order to evaluate the content of oxygen in HTS samples, but all of those measurements result to be destructive, which means that once the characteristics are analysed, the sample is no longer useful. Because how close the superconductivity in oxygen deficient perovskite is in a relation to the crystal structure, a non-destructive method to evaluate the oxygen quantity in HTS

seems to be more appropriated. The method followed in this project is more detailed in section 1.2.

### 1.1.3 General consideration of YBCO as a High Temperature Superconductor:

These materials, which present superconducting properties, have their critical value of some variables from which they stop acting as superconductor. An easy manner to explain this is following the figure 4 where it can be seen the critical surface in temperature-magnetic field-current density phase space [18]. From this three dimensional system, the x-axis correspond to applied field (H), the y-axis with the temperature (T) and the z-axis with the current density (J). When these parameters are less than the critical values,  $H_c$ ,  $T_c$ , and  $J_c$ ; the material acts as a superconductor. In the case that any of these variables exceeds the critical value, the material would be found in its normal state.

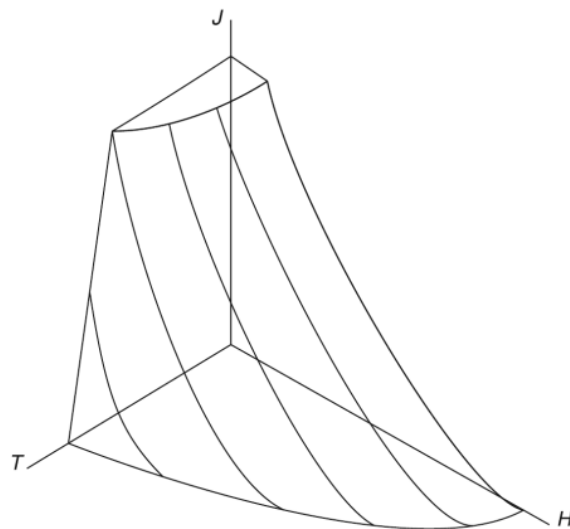


Figure 4. Diagram of the critical surface for superconducting properties.

Following a thermodynamic transition, so it can pass from superconducting state to the normal one, a variation of energy equal to  $\mu_o \cdot H_c^2 \cdot \frac{1}{2}$  is achieved. This corresponds to the condensation energy. Even the critical current density is not a thermodynamic phase transition parameter; it is considered a key parameter for many applications.

The resistivity can be roughly defined as the specific resistance a material shows for the flow of electric current and it can be expressed as  $\rho = R \frac{S}{l}$  ( $\Omega \cdot m$ ), where  $R$  is the resistance ( $\Omega$ ),  $S$  is cross section area ( $m^2$ ) and  $l$  is the length (m). A comparison of the resistivity with the temperature between a normal metal and a superconductor material can be illustrative to show different dependence. A decrease on the electron scattering from phonons in the metal can be expected as the thermal lattice vibration decreases. If the superconductor is under normal condition of temperature ( $T > T_c$ ), this presents a similar behaviour, but if the temperature is higher than the critical value, the material shows a condensed electron state, which allows zero resistance for direct current.

The induced magnetic moment per unit volume as response of a magnetic field applied ( $H$ ) is known as the magnetization and it is denoted by "M". As it can be found in many literature reviews the classification of superconductor materials can be realized depending on different criteria, being one of them their physical behaviour, which divided these into superconductors type I or type II. A comparison between these two kinds can be shown in the graphic below, where is represented the magnetization dependence with the applied magnetic field [18].

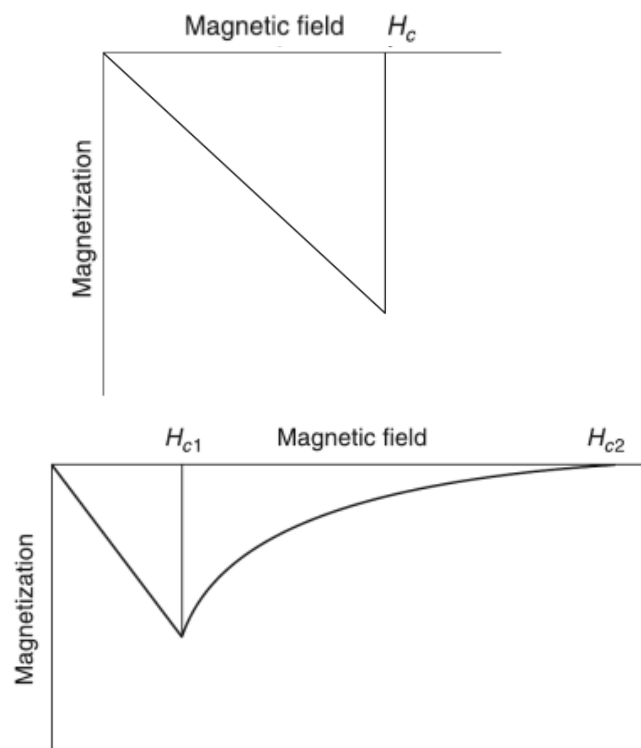


Figure 5. Magnetization as a function of a magnetic field applied in a Type I (top) and Type II (bottom)

In the case of the Type I superconductors, it can be observed that the magnetization is equal and opposite to the magnetic field, which leads to a truly zero magnetic flux density (B) inside the superconductor, following the expression  $B = \mu_0(H + M)$ . This expulsion of all magnetic field is known as the *Meissner Effect* and it corresponds to a perfect diamagnetism, which was considered a key property for superconductors until in 1937, Shubnikov et al. presented superconducting alloys which magnetization didn't respond the same way as it is shown in the figure 5 (top). After many researches and studies, a curve explaining this new type of superconductors was realized and it is shown in the bottom of the figure 5. This graph represents the response in a Type II superconductor when a magnetic field is applied. As it can be noticed, this kind remains a perfect diamagnet until it reaches its lower critical field value,  $H_{c1}$ . After this value, it does not stop being superconductor, as in the previous case, but remains superconducting until its upper critical field,  $H_{c2}$ . Between these two values,  $H_{c1}$  and  $H_{c2}$ , the material still a diamagnetic but not a perfect one. When the applied field increase, the density of fluxons increase until at  $H_{c2}$ , when a full field penetration is achieved and it starts the material transition to its normal state.

A fluxon is a quantum of magnetic flux, which is formed in Type II superconductors when a magnetic field incident on the superconductor surface creating a small non-superconducting region. Around this region a small electrical current is circulating, which leads to the formation of fluxons that are threaded through single cores of normal material. These cores are known as vortices. A regularly spaced vortex lattice forms, which lattice spacing is inversely proportional to H, being zero when its value is close to  $H_{c2}$ , which correspond to the full flux penetration and also to the variation to the normal state

When the Type II superconductor state is found in between  $H_{c1}$  and  $H_{c2}$ , a resultant Lorentz force can be observed:  $F_L = J \times B$ , where B is the magnetic flux density and J the current density. This force acts transversely on the vortices and its vector is perpendicular to the current and also to the vortices. If there is no found any restraining force on the vortices, these will be moving through the material, phenomenon that is named flux flow and which is the cause of possible dissipation.

The onset of this flux flow determines the value of the critical current density,  $J_c$ . The stronger the interaction of defects with the vortices as well as the closer the match between the defect and vortex spacing, the higher is the resultant pinning force,  $F_p$ . For high value of the pinning force, great energy is required to move the vortices in or out of the material.

Type I are found only in pure elements being approximately thirty elements, which show this behaviour. Type II superconductors, which is the one that define the material used for this project, YBCO, can have high values of  $H_{c2}$ . This makes them the most adequate for practical applications and they are commonly utilized for commercially use.

Unlike the low temperature superconductor materials, High temperature superconductor have a vortex liquid phase when  $H$  and  $T$  are high, so they show greater thermal energy at the high values of the transition temperature,  $T_c$ . Between the vortex solid and the liquid states vortex it is formed a boundary named the irreversibility field,  $H_{irr}$ . This parameter is the one that will determine the upper limit for  $J_c$  in the case of HTS, instead of the theoretical well-known,  $H_{c2}$ . This study is still not well defined by previous literature review and it demands more investigation in order to understand the dependence of this parameter with  $F_p$  or  $J_c$  [18].

#### 1.1.4 Anisotropy and grain connectivity:

High temperature superconductors (HTS) materials exhibit a strong anisotropy in their crystallographic and also in their superconducting properties. The three crystallographic axes that these materials show are “a”, “b” and “c”. This last axe is directed normal to the cuprate planes, where the other two are found. In the case of YBCO, as it is an oxide superconductor, the anisotropy in a-b can be considered neglected as it is normally small enough to do so, whereby this material may be treated as being uniaxial [19].

In a polycrystalline superconductor it has been demonstrated that the anisotropy in  $J_c$  have serious consequence, providing high limitations on current flow, in the case that all grains are not aligned with each other and as well if there are no well aligned with the direction of the current flow. For the superconductor material it is going to be studied in this project, YBCO, it can be observed a precipitous drop in the critical current density,  $J_c$ , for mis-orientation angles greater than  $2^\circ$ , which means that any manufacturing method must produce long lengths of conductor presenting aligned grains to within a few degrees in order to take advantage of the intrinsically high  $J_c$  in this superconductor material. For the case of YBCO, bi-axial texture is recommended, which means that not only the crystallographic c-axes must be aligned but as well the axes within the  $ab$  plane.

In the figure 6 can be observed the variation of  $J_c$  that can be found on a sample of YBCO with the angle between the applied field (denoted by  $H_{\parallel ab}$  for the parallel field to  $ab$  plane) and the orientation of the sample.

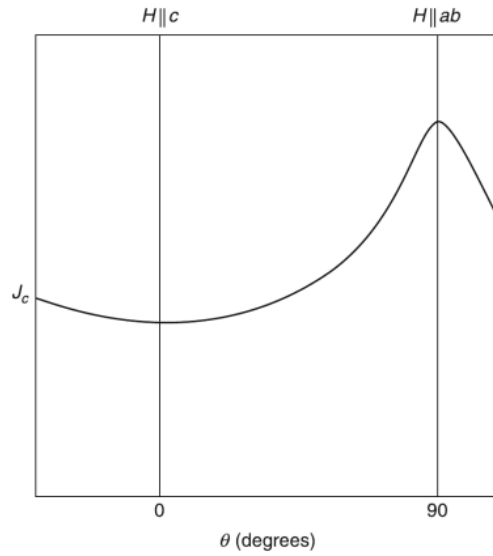


Figure 6. Example of the variation of  $J_c$  with the angle between applied field and the orientation of the sample in YBCO [19].

The high anisotropy from the fact that superconductivity occurs generally in the  $\text{CuO}_2$  planes and it can be reached weak interlayer couplings between them is normally denoted by the dimensionless parameter  $\gamma$  and it is defined as:

$$\gamma = \xi_{ab}/\xi_c$$

Where  $\xi_{ab}$  and  $\xi_c$  correspond to the superconducting coherence length, which are parallel or perpendicular to the plane  $ab$ , respectively.

Beside this, in the case of YBCO, it is found dependence to several physical properties with parameters like temperature and frequency of the applied electromagnetic wave, which has been demonstrate to have a directional aspect. This anisotropy is generally attributed to the orthorhombic crystal structure and the existence of the  $\text{CuO}$  chains along the  $b$  axis [20].

Abbreviation	Compound	Space group	Lattice parameters (Å)		
YBCO-123	YBa <sub>2</sub> Cu <sub>3</sub> O <sub>7-x</sub>	<i>Pnmm</i>	<i>a</i> = 3.8227	<i>b</i> = 3.8872	<i>c</i> = 11.6802
YBCO-123	YBa <sub>2</sub> Cu <sub>3</sub> O <sub>7</sub>	<i>Pnmm</i>	<i>a</i> = 3.8185(4)	<i>b</i> = 3.8856(3)	<i>c</i> = 11.6804(7)
YBCO-123	YBa <sub>2</sub> Cu <sub>3</sub> O <sub>6.8</sub>	<i>Pnmm</i>	<i>a</i> = 3.8214(7)	<i>b</i> = 3.8877(7)	<i>c</i> = 11.693(2)
YBCO-123	YBa <sub>2</sub> Cu <sub>3</sub> O <sub>6.56</sub>	<i>Pnmm</i>	<i>a</i> = 3.8336(4)	<i>b</i> = 3.8807(4)	<i>c</i> = 11.7355(10)

Bond lengths (Å)					
YBCO-123	Cu1–O1	1.836	1.876	1.848(4)	1.857
	Cu1–O4	1.944	1.921	1.926	1.944
	Cu2–O1	2.306	2.293	2.302(5)	2.296
	Cu2–O2/3	1.946	1.931	1.944(1)	1.946
	Ba–O1	2.744	2.735	2.744(1)	2.742
	Ba–O2/3	2.972	3.168	2.951(5)	2.976
	Ba–O4	2.879	2.835	2.908(3)	2.879

Figure 7. Data of several lattice parameters collected by Koblishka-Veneva et al. [20]

### 1.1.5 Thermal properties:

In the case of YBCO, some peculiar features are found if a comparison with the convectional superconductor materials is realized. Some anomalies, such as the fact they are the finite  $\gamma * T$  term in the superconducting state, the improvement of  $C_p/T$  and anomalous peak shape around the transition temperature,  $T_c$ , and at 220 K, are resulting very interesting for many research groups as it can provide information so a full understanding of the mechanism of this HTS can be achieved [21].

Base in different reports where it can be found heat studies on YBCO, the data are well approximated by the following expression (1) for analysis in temperature range from 1.4 to 7K and (2) for temperatures above 8K [22, 23]:

$$(1) \quad C_p(T) = \gamma * T + \beta_3 \cdot T^3 + \beta_5 \cdot T^5$$

$$(2) \quad C_p(T) = \gamma * T + \beta_3 \cdot T^3$$

Where  $\beta^3 = (12/5) \cdot \pi^4 \cdot R \cdot \theta^{-3}(0)$  in the case of (1) and  $\gamma * = 0$  and  $\beta = 0.60 \text{ mJ}/(\text{mol K}^4)$  in the case of (2).

The anomaly at temperatures around 220K in YBCO has been normally attributed as structurally related origin [24]. The oxygen content effect on the  $T_c$  is well known nowadays and the connection among the 90 and the 220 K anomalies suggest that the order on the oxygen may be the cause of this anomaly at 220 K.

Another basic thermal characteristic of copper oxide superconductors is the poor thermal conductivity,  $\kappa$ , they usually have [21]. Base on experimental data collected from studies of the thermal conductivity of YBCO can be noticed that the results for  $\kappa(T)$  of the Y-123 compounds at temperatures lower than 10 K show high variations depending on the microstructure of the sample, oxygen content, admixture and on the crystallite borders as it can be seen in the following figure:

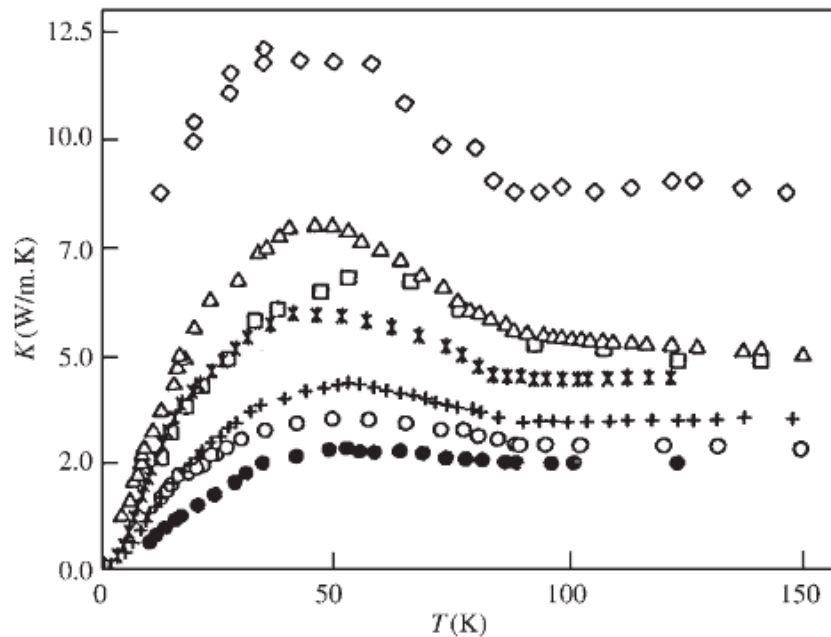


Figure 8. Thermal conductivity vs. temperature for different samples of  $YBa_2Cu_3O_{7-x}$  [25]

### 1.1.6 Mechanical properties:

Mechanical features of high temperature superconductors are important for engineering applications as these materials are considered brittle and sometimes even fracture. Because of this, improvements of mechanical properties are generally carried out for practical applications as thermal stress and electromagnetic force during superconductivity operation can be found.

Because of the variation in the thermal expansion coefficients between the contacts of different phases, cracking in ceramics is normally presented. This thermal expansion coefficient, denoted by  $\alpha$ , can be defined as the variation of the length or volume per degree of temperature.

$$(3) \quad \alpha = (dl/l) \cdot dT$$

$$(4) \quad \gamma = (dv/v) \cdot dT$$

The first equation (3) corresponds to the coefficient of the line thermal expansion, where  $l$  is the length; and the second one (4) to the volume thermal expansion, where  $v$  is the volume. In both cases,  $T$  corresponds to the temperature and even they both depend on it, the coefficient value generally used is the mean value averaged over a determined temperature range [27].

The amplitude of the atomic vibration at equilibrium position experiments an increase with the temperature, which lead to an increase in the bond length and also in the lattice expansion. The variation of the volume with the lattice vibration leads to an increase in the free energy of the lattice. Therefore, at low temperatures, a strong increase of the thermal expansion coefficient with the temperature can be demonstrated, remaining almost constant for temperature above the Debye one, assuming the lattice simply expands. This fact doesn't happen in all HTS, through the formation of lattice defects, for some of them the thermal expansion coefficient can increase even above Debye temperature.

Fracture toughness is also important to take into consideration for mechanical properties. It reveals the resistance the sample shows against crack propagation. Generally, the techniques used to characterize this parameter for brittle materials like HTS ceramic materials are the Vickers indentation (ID) method and single-edge notch beam techniques (SENB).

As a comparison to metals, high temperature ceramic superconductor materials are very brittle and they can fracture even at elastic limit, which can be attributed to the absence of multiple active slip systems. The tensile strength is defined as the stress at which the body breaks, attributed when stressed in tension. When stressed in bending are called flexural strength and when stressed in compression, compression strength. The strength parameters generally depend on the amount of defects and a bending test is normally used to estimate the fracture strength for brittle materials. In the case of Y-123, the fracture strength reported is in the range of 40 to 200 MPa [26]. The possible variation of this value is attributed to the porosity density, oxygen content and/or amount of cracking.

As it can be noticed in figure 9 [27], YCBO deforms more than 50% for temperatures above 840 °C when compressive strain. A gradually decreased of the flow stress is showed as the deformation proceeds once it is reached the yield in temperature from 840 °C to 900 °C.

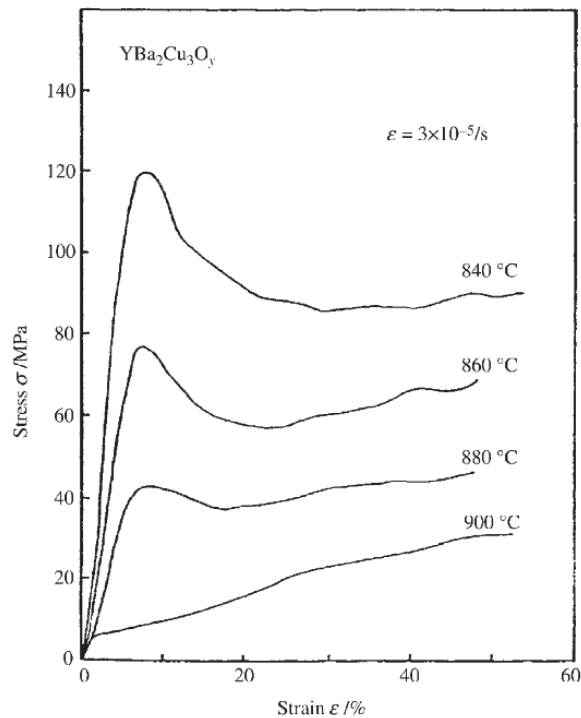


Figure 9. Curve of stress-strain for the HTS material Y-123 in compression above 840 °C

### 1.1.7 Applications of HTS:

It is well known nowadays all the large scale applications the high temperature superconductors can be involve in, such as power transmission lines, energy storage devices, fault current limiters, motors and electric generators, medical devices or applications in particle accelerators [28]. But the applications that are going to be pointed out for this project are the possible small scale ones, as the process to study is based on the micro manufacturing technique, Micro-FAST. The most attractive applications of HTS small-scale devices can be summarised in two main classes, SQUID systems and Josephson devices.

#### 1.1.7.1 Superconducting Quantum Interference Devices:

SQUIDs systems are design specially to measure the magnetic flux and some other electromagnetic measurements. They are considered one of the most sensitive detectors of magnetic flux. It can be said that converts variations in a physical quantity, i.e. a transducer, which produce voltage proportional to the magnetic flux.

This device is able to combine to physical phenomena: flux quantization and tunnelling [29]. Magnetic flux quantization is considered a closed loop in the bulk of a superconductor and the quantum mechanics must be applied for the superconducting state,

so applying the Bohr-Sommerfeld quantization rule to the loop mentioned it can be obtained the equation (5) where it can be observed a relation between the linear momentum  $p$ , the line element  $d\vec{l}$  and the Planck's constant  $h$

$$(5) \quad \oint \vec{p} \cdot d\vec{l} = nh$$

where  $n$  is a line element.

The value of  $p$  can be obtained with the equation  $p = mv + qA$ , where  $m$  corresponds to the mass,  $v$  to the velocity,  $q$  to the charge and  $A$  to the vector of the magnetic potential. If this equation and the rotational theorem are used in (5), considering the velocity with a zero value in the bulk of the material, the following equation can be obtained

$$(6) \quad \iint \text{rot } \vec{A} \cdot d\vec{S} = nh/q$$

Here  $d\vec{S}$  corresponds to an area element. As it is known  $B = \text{rot } A$  and also that  $q = 2e$ , so the equation (6) can be expressed as

$$(7) \quad \Phi = \iint \vec{B} \cdot d\vec{S} = nh/2e$$

Which equation is the flux quantization rule, i.e. the magnetic flux, denoted by  $\Phi$ , must be quantized in superconducting loop following the rule  $\Phi = n\Phi_0$ , being  $\Phi_0 = nh/2e = 2.07 \times 10^{-15} \text{ Wb}$  [28].

In conclusion, a SQUID is a closed loop superconductor, which contains one or more Josephson junctions. This allows us to measure quantities smaller than  $10^{-15} \text{ Wb}$  as it is a flux-to voltage transducer which produces voltage proportional to magnetic flux. The devices based on SQUIDS are nowadays the most typical and appropriated ones to be used when a high precision in the electric and magnetic measurement want to be obtained.

SQUIDS can be divided in two different types, *dc SQUID*, which is based in two Josephson junctions, connected in parallel as it can be observed in figure 10 and it works with steady current bias; and *rf SQUID*, which consist in one Josephson junction that interrupt the flow of the current found around the superconducting loop and operates with a rf bias. The illustration of figure 11 shows an rf SQUID system.

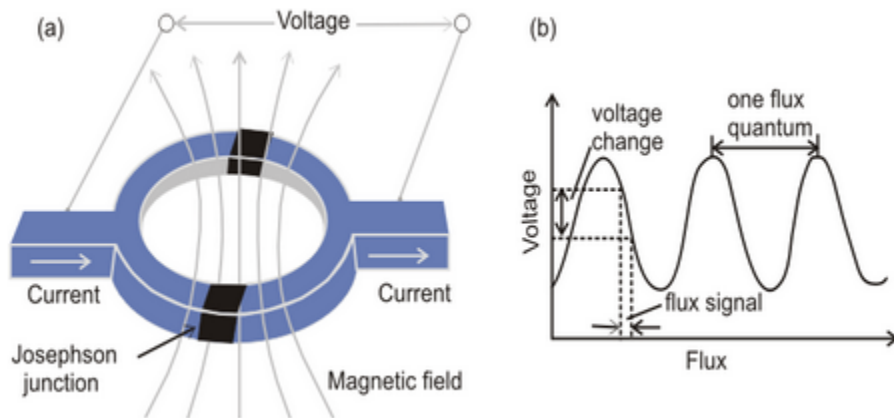


Figure 10. Example of a dc SQUID [30].

In the figure above it can be observed the Josephson junctions forming the superconducting closed loop, which forms the dc SQUID (a) and also the output voltage in relation of the applied flux (b).

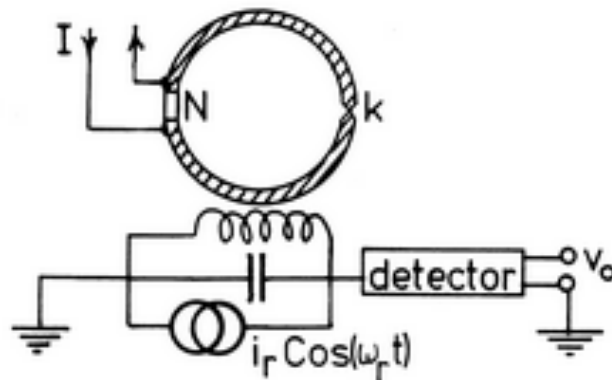


Figure 11. Schematic of a rf SQUID system.

As this system only requires one Josephson junction it is simpler to fabricate and it can be found in the market nowadays. However, it has been demonstrated that dc SQUIDs are more sensitive, so the possible improvement and development of this kind has caught all the attention in the last decade.

SQUID systems can be used for a large number of practical applications, such as the detection of submarines or relative motion magnetic field, medical diagnostics, mineral survey, etc. [28].

### 1.1.7.2 Josephson junction devices

The superconductor devices based on Josephson junctions are considered the most important for small scale. There can be identified two different Josephson junctions from the practical point of view of Josephson effects:

- Superconductor – Insulator – Superconductor (SIS) junction. They are also known as tunnelling junctions as it occurs tunnelling of the Cu pairs among the superconductors through the barrier of the insulator [29].
- Superconductor – Normal – Superconductor (SNS) junction. In this type of junction does not exist an insulator barrier but just two interfaces SN.

The characteristic curve of the current – voltage of a SIS junction will be different from the one of the SNS junction, a theoretical prediction of this curve can be observed in different reports (Kummer et al. 1990) where it can be seen that it exhibits a negative resistance region. It can be demonstrated that SNS junctions are more appropriate than SIS junctions for small scale applications of superconductivity with HTS [28].

### 1.1.7.3 Electronic applications:

A new kind of electronics based on superconducting devices can be observed in the last decade to be a promising way of improvement in the performance of traditional semiconductor electronic devices, which were the most modern and reliable technology since 1950. The main important improvement in electronic applications with superconductor materials is the speed limit explained by the Joule's law

$$(8) \quad Q = R \cdot I^2$$

Where  $Q$  corresponds to the heat loss,  $R$  to the resistance and  $I$  to the current. If it is used a superconductor instead of a metal, the metallic interconnections can be avoided, so the speed of the processors, among other devices, can be increased.

Some interesting applications have been presented by the military in the USA based on the use of HTS material filters in aircraft electronics. They believe a better rejection of the interference noise in radar systems can be obtained. For some mobile phone with HTS microwave filter subsystem, which can be nowadays found in the US market, it has been noticed some improvement in the noise data, the radio frequency coverage in rural areas with a smaller number of base stations or even reduce the radio frequency power of the mobile phones in urban areas [31].

The determination of signal forms with ps resolution is possible nowadays in Josephson samplers, as the fast voltage reaction of a Josephson junction on a signal current,

which surpass the critical current, allows this. A high temperature superconductor Josephson sampler system at NEC has demonstrated a resolution of 5.9Gbps digital waveform [32].

HTS it is been also used for the fabrication of superconducting AD converters, they are useful for this because the periodicity of the electric properties of superconducting loops as a function of the magnetic flux. The quantization of the flux can lead to a feedback loops implementation with quantum accuracy [33].

Other applications where it can be used superconducting devices based on SIS junctions and SNS junctions can be used as substitutes of semiconductor devices, such as generators, amplifiers, mixers, detector, switches, etc. [28].

## **1.2 Process:**

### **1.2.1 Obtaining Powders.**

The control of the physical and chemical properties and aspect of superconducting materials is one of the main objectives in the chemical processing of HTS, as the grain connectivity plays an important role for practical parameters that need to be control for advance application, leading the physical properties of HTS be highly dependent on their chemical processing [34].

The intrinsic values that must be considered for a good characterization of these materials, and more specifically their anisotropy, speaking of physical parameters, are only accessible, directly, from single crystals. The preparation of high temperature ceramic superconductor materials requires the control and reproduction of the features of the final product starting from the powder products, so a precise control of the properties presenting on the powders by a chemical approach can be considered an essential condition for the manufacturing of HTS components.

In order to obtain the best results from the sintering process an analysis of the physical properties must be taken into a count. The main principle physical properties of high temperature precursor powders can be classify as:

- *The size distribution.* It can be determined by different methods, such as laser diffusion, which can give an average of the particle size distribution, estimating the particles are spherical; gravity sedimentation, which is based on the relation within the sedimentation velocity that the particles suspended in fluid have and the viscosity presented on the

medium; optical or electronic microscopy, etc. This last one is the one is going to be used in our experiment and the results are showed in section 4.

- *The degree of aggregation and the morphology of the grains.* Because of these factors, the average value of the particle size distribution can vary from one batch to another. Depending on which is the size range and the level of resolution, different microscopy techniques are found to be the most preferred.

The chemical composition is also another factor that must be considered for the analysis of the samples. Several techniques are known, nowadays, to be appropriated to study and determine the chemical phase composition that is seen in the powders, depending, mainly, on the concentration of the secondary phases or/and impurities. The most relevant techniques are inductively coupled plasma (ICP), X-ray fluoresce spectrometry and electron-probe micro-analysis (EPMA) and X-ray powder diffraction (XRD), among others [34]. This last is the one is going to be used for the chemical analysis in this project. It is based on the diffraction lines analysis, which lines are produced by the interaction among a monochromatic X-ray bean and the powder. The position of the different diffraction lines represents the crystal structure; however the atomic composition can be related directly with their scattered intensities.

### **1.2.2 Synthesis processes:**

The first step of the sintering process consists on the preparation of good quality starting (precursors) powders. The synthesis process carried out for the production of the powders is a very important step to take into account before study the sintering process and it can be found a large variety of routes. It has been demonstrated that the characteristics of the powder, and also of the final product, are often reflected by the preparation technique employed. It is the step where can be achieved an improvement of the processibility, an enhancement of the current carrying capabilities of the superconducting materials by improving the chemical homogeneity and the following manufacturing steps, enhancing also the mechanical properties. It also helps to understand and investigate the influence that impurities have on the superconducting features.

These techniques can be classified into three main categories [35]:

- *Solid-state synthesis.* This procedure takes into consideration the physical features of the reactants and the chemical reactions that are involved. The most old method use commonly is the conventional ceramic process, which uses a mix of reactant followed by a formation of a phase. Another subcategories from a solid-state synthesis are the metallurgical route, which uses metal powders instead of metal compounds; the alkali flux process, which work with an alkali bath of NaCl, Kcl or Ba(OH)<sub>2</sub> for the mixing of the precursor metal compounds;

and the solid-state combustion synthesis, where the exothermic chemical is performed in order to obtain the phase formation.

- *Solution techniques.* A large number of different solution techniques can be found in previous reports, such as solution-drying method, using an aqueous solutions of metal salts dried so an homogeneous mixture of constituents can be achieved; Coprecipitation process, the cations are normally precipitated from solutions as hydroxides or carbonates or like complexes of organic legends; sol-gel process, where the cations first form a sol of hydroxides or citrates or even acetates; spray-drying method, which involves spraying an aqueous solution of the cations in the form of small fine drops into a heated chamber; or freeze-drying methods or aerosol process, among others.

- *Vapour/plasma process.* This procedure has become very popular in the past decade for the production of ultrafine ceramic powders. The precursor solution is injected into plasma and then the collection of the particles is carried out.

For this project the Yttrium Barium Copper Oxide (1-2-3) powders has been supplied by the company Alfa Aesar were the powders were prepared from an intimately mixed precursor powder, made by a Coprecipitation method. This method is based on the formation of crystalline or amorphous solid phase with the stoichiometry appropriate through the precipitation of the reactant ions from a solution. The control of the stoichiometry is the main difficulty of this route; this is why the precipitating agent must be an organic compound, multivalent, in coordination with more than one metal ion. It is also needed that the precipitate is insoluble in the solution so the separation of the solid precursor and the solution.

The main advantage of this method, compare to others, e.g. solid-state synthesis, is that reactant ions are fond mixed at a molecular level, which leads to a better homogeneous distribution of the reactants in the starting powder of the superconducting materials. After this, a decrease in the temperature of the reaction and also in the time used for the annealing process is generally observed, due to the significantly reduction of the diffusion barriers compare with others convectional synthesis processes. Small particle size and low degree of aggregation, which will help the final product to show a high density, can be obtained due to the easy thermal decomposition of the precursor controllably [34].

An example of a standard route followed in a co-precipitate synthesis route can be observed in the figure bellow.

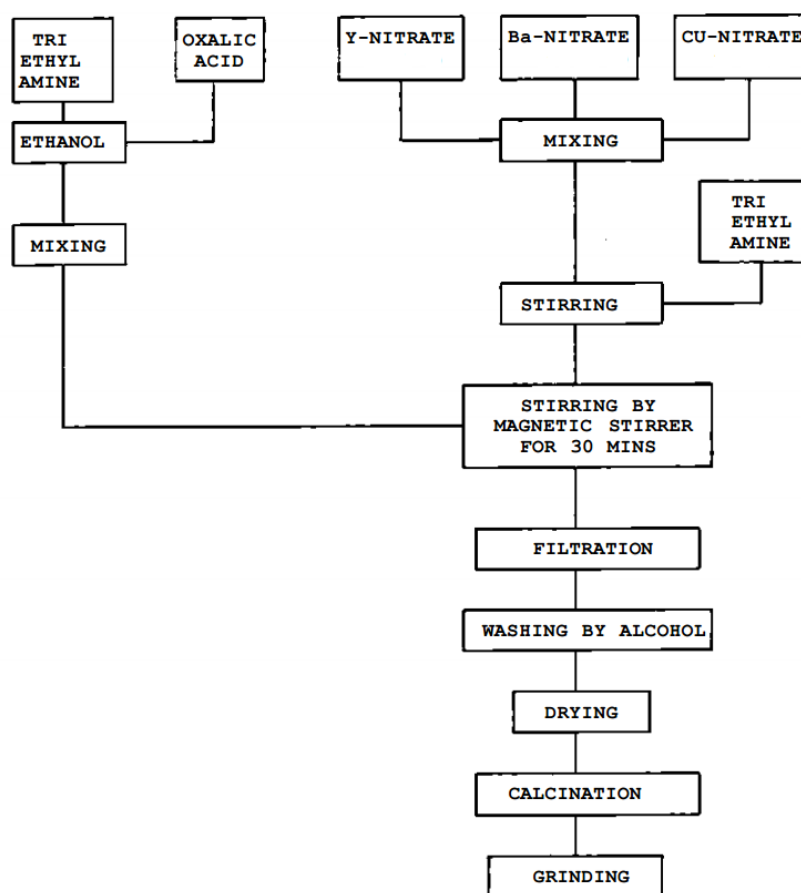


Figure 12. Example of a flow diagram for the preparation of YBCO powders [36]

The information given by the suppliers ensure that the process avoided any sequential precipitation of metal ions in order to achieve the stoichiometry. Solution based methods were used to improve homogeneity, purity, and reduce particle size. They also guarantee that the metallic salts were dissolved in water and then precipitated and that the anion solution used simultaneously precipitates the cationic species as carbonates and/or hydroxides. The phase pure, low carbon superconducting powder was produced by a low pressure calcination process. The low processing temperature resulted in powders of a fine particle size and the homogeneously mixed precursors increased the reaction rate during calcination.

### 1.2.3 Sintering Process:

#### 1.2.3.1 Theory:

Sintering can be defined as the process where powder compacts are transformed into coherent and predominantly solid structure with the application of heat. It is a process where the powder particles bond together by different atomic transportation mechanisms and where somewhat porous body acquires a certain mechanical strength. From a microscopic point of view, this bonding occurs as connection necks grow at those points where the particles are in contact. As these bonds among the particle interfaces become larger and start combining, a grain growth and a densification proceed [37].

Sintering is considered one of the most important processes in the manufacture of ceramics from powders to fabricate a shape product with a desired property, structure, dimension and/or tolerance. A large development of nanotechnology as well as the extensive application of science and engineering of different materials at nanoscale level, has led to new possibilities and challenges in the sintering processes [38]. A rational theory of sintering is defined in order to predict the routes followed for the fabrication of the desired structure of a sintered sample, which are determined by its physical, chemical and mechanical properties can be provided [39]. Therefore, the objective of the study of the sintering is to understand the influence of different variables, such as the temperature, the particle size, the pressure applied, the particle packing, the atmosphere and the composition of the powders.

A classification of four groups of sintering can be found in different reports [40]:

- *Solid-state sintering*: It is the process where it is normally used 0.5 or 0.9 of the melting point as the sintering temperature to heat the green body. There is no presence of any liquid phase and the join of the particles and the decrease of the porosity are mainly produced by the atomic diffusion in the solid state.
- *Liquid-phase sintering*: In this process, at the sintering temperature, a little amount of liquid phase can be found, generally less than a small volume percent of the precursor. This method is considered one of the most important methods for industrial fabrication of several ceramics as it enables the densification at low temperatures.
- *Vitrification*: Vitrification refers to the glass formation. In this method, typically, more than the 25% of the original volume of the solid is found in a liquid phase formed on heating, which is enough to fill the pores remained in the body. With this process, a dense sintered sample can be obtained by the formation of the liquid, the flow of this liquid into pores and also by crystallization or vitrification of the liquid on quenching. This method is generally used when the raw material is naturally available, such as clays.

- *Viscous sintering*: The sintering temperature typically used in this process to consolidated mass of glass particles is similar or above its softening temperature, allowing the densification by viscous flow of this glass under the surface-tension's influence.

It has been demonstrated that for some conditions, the used of any of these four methods is not good enough to achieve the desired properties on the body. This is why, the combination of these processes with the simultaneously application of pressure, even it results an increase of the fabrication cost, is demonstrated to be an effective method when a high density and fine grain size is desired in the microstructure. The sintering processes without the application of pressure are known as convectional sintering and the one using pressure when heating non-convectional sintering, which is the one used for this project.

#### **1.2.3.2 General considerations:**

After a sintering process, an increase on the volume fraction of 50%, compare to the compacted powder into green body, can be achieved. Henrring's Law [41] presented by Terpstra et al. established that, in order to obtain good sinterability, the ceramic powder used for a sintering process must be fine, pointing out that if a smaller particle size of the powders is used, the sintering time to obtain a determined density is reduced. Another factor that must be taken into account is the free from agglomerates of the powders, otherwise differential sintering, inhomogeneities and trap internal stress can be produced [42].

The initial stage in the sintering process, which determined to be by evaporation and condensation, can be explained with the scheme showed in figure 13. [43]. A driving force is provided by the difference found in the free energy or in the chemical potential among the area where the neck is formed and the surface of the particles. This causes a material transfer by the fastest medium possible. If the vapour pressure is not high enough, it can be other solid-state processes by which can occur the material transport. The relative rates that these processes present in a particular system, is what determine which are dominant in the sintering and not all of them result in a reduction in porosity. The transfer of matter from the volume of the particle or grain boundary among the particles is the only one that causes shrinkage and pore elimination.

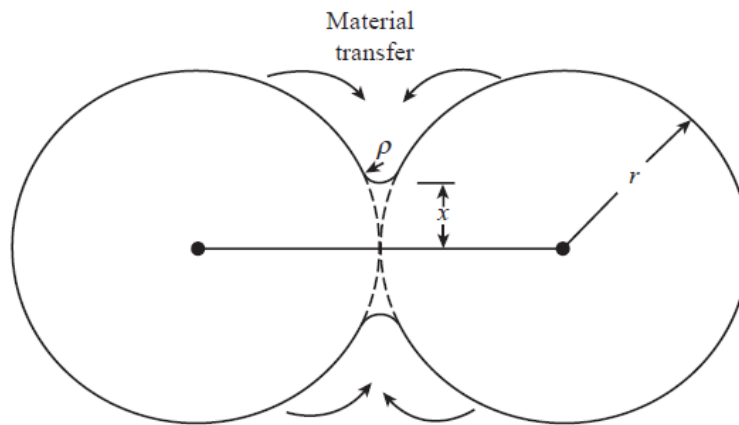


Figure 13. Representation of the first stage of the sintering process

As it has been briefly described above, different categories can be defined to classify the sintering processes. For the case of HTS materials, the two main ones are the solid state and the liquid phase sintering.

In the solid-state diffusion, the vacancy migration is generally the rate-determining step. To be able to describe this, a relation between the surface energy, the volume of the lattice vacancy, the diffusion coefficient and the time; must be determined, taking into account the high anisotropy with regard to diffusion and the mass transport essentially taking place in the a-b plane, that all HTS present [43]. The other typical process used for HTS, the liquid phase sintering, a rapid material transport and densification can be achieved as the presence of the liquid phase improve the diffusion and can arise through thermodynamically driven phase variations as the material is heated, or even being added as an extra component to the compact of the powder prior the sintering. However, because of the high influence the structure and morphology of grain boundaries has on the HTS materials properties, the addition of grain boundary phases in the final sintered product is generally avoided. For the case of this last method, because of the presence of the liquid phase, a relation with viscous flow can be applied [44].

### 1.2.3.3 State-of-the-art of sintering process for YBa<sub>2</sub>Cu<sub>3</sub>O<sub>x</sub>

In order to produce sintered samples with the desire shapes and properties for specific applications and also for assessment, characterization and scientific study, it has been carried out much work regarding the sintering process of YBa<sub>2</sub>Cu<sub>3</sub>O<sub>x</sub> [45]. A large number of different sintering techniques can be found in previous research papers and literature reviews. For this material, it has been observed that the most used methods are

the conventional powder pressing techniques, where these powders are placed in a die and, applying a pressure on the punch, it can be obtained a dense body.

Different factors, such as the size of the particle, the size distribution of the powder or the pressure applied, are known to have a big influence in the green density of the compact powders. As it is an irreversible process, sintering is accompanied by a lowering of the system free energy, which sources that produce this are normally referred to as the driving force for sintering. There are three possible driving forces: the curvature of the surface of the particle, the external applied pressure and also the chemical reaction [46]. Pressure sintering can lead to acceleration in the nanoceramic densification and the achievement of nanosized grains by giving external sintering driving force [47]. This applied pressure can lead to obtain fully dense samples using lower sintering temperature and/or shorter sintering time. However, the use of pressing pressure has its limitations regarding the ability in forming complex shapes and can lead to higher cost. Another consideration that must be taken into account is the anisotropy that may be found on the densified microstructures. The typical pressure applied for this HTS is around 100MPa, but some other reports can be found, where it was able to obtain sintered samples with pressures in a range from 15 to 45 MPa when the combination of current and heat is acting [48]. It is well known that a higher pressing pressure can generate cracks and defects once this pressure is released. In order to improve the strength and handleability of the powder compact, some amount of polymeric binders (around 1% by weight) can be added during the final stages of the preparation on the precursor powders. Different uniaxial pressing techniques can also lead to density variations throughout the compact, generally due to the friction happening between the die's wall and the powders [45]. These variations in the density can lead to non-homogeneous sintering and also to distortion of the final product.

The heating rate is another important parameter to take into consideration when a sintering process is going to be performed. Many factors can affect the sintering rate of YBCO, such as particle size of the precursor powders, sintering temperature and time and also the atmosphere where the process is taking place. As it has been mention in section 1.1.2YBa<sub>2</sub>Cu<sub>3</sub>O<sub>x</sub> shows a relative weak-link compare with other HTS, which are known to give several limitation on the J<sub>c</sub> values of superconductors. The reasons for theses weak links are attributed to misorientation of grain boundaries and variations on the composition at the grain boundaries [49]. It can be observed that the atmosphere can also modify the weak-link behaviour of YBCO superconductors. An example of the influence of the atmosphere in the critical current density can be observed in figure 14. Beside the atmosphere, as it has been mentioned above, the particle size also affect to the sintering process. The use of coarse powders gives the produced samples a higher porosity and large particles, i.e. poorer sintered samples. However, if the grinding time is increased in the preparation process of the powders, finer particles can be obtained and higher dense final product can be achieved.

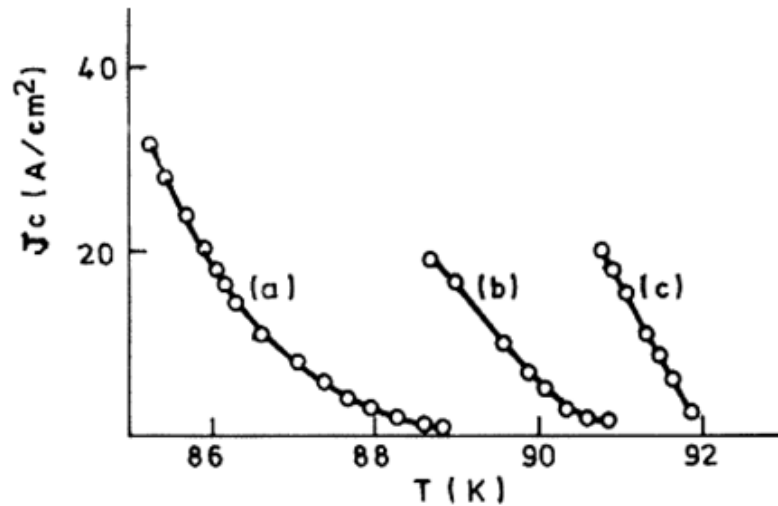


Figure 14. Variation of  $J_c$  with the temperature for different atmosphere: (a) oxygen, (b) air and (c) argon atmosphere [49].

The dimensional shrinkage that occurs in the samples during the sintering process and also the linear shrinkage parameter  $\delta L/L_0$ , which is also known as the densification parameter,  $\alpha$ , are related to the densification of the sample. The porosity of the compacts shows a systematic decrease with both the sintering time and the sintering temperature, this lead to the conclusion that the densification parameter depends also on the time and temperature [50]. This densification parameter,  $\alpha$ , can be related with the sintering variables as it can be observed in the following equation [51, 52]:

$$(9) \quad \alpha = \left(\frac{K'}{T}\right)^n \cdot e^{-nQ/RT} \cdot t^n$$

From this equation,  $Q$  correspond to the activation energy for the rate that regulate the step in the sintering process;  $n$  is the parameter of the sintering kinetic,  $R$  is the gas constant,  $t$  is the time,  $T$  is the temperature used in the process, expressed in K and  $K'$  is a constant. It is more common to express this equation in terms of logarithms:

$$(10) \quad \ln(\alpha) = n \cdot \ln(K') - n \cdot \ln(T) - \frac{nQ}{RT} + n \cdot \ln(t)$$

In this case,  $n$  can be obtained if it is plotted  $\ln(\alpha)$  vs.  $\ln(t)$  at different temperatures and in consequence the activation energy could be calculated using the equation (10). An example of this variation of the sintering parameter,  $\alpha$ , with the sintering time used can be observed in the figure below, which is an image from a report carried out by L.C. Pathak et al. [50].

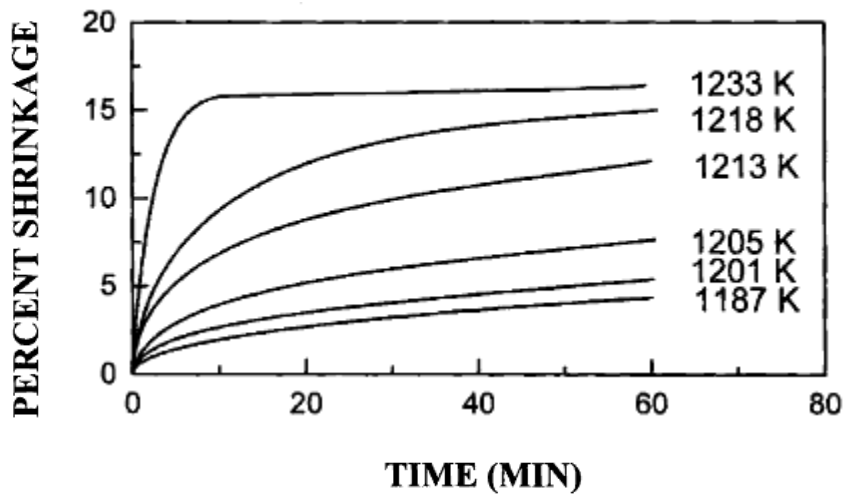


Figure 14. Example of the variation of shrinkage with the process time performed at different temperatures.

Even it is not our case, we can see as a reference how the variation of linear shrinkages with the time spent in the sintering process shows a continuous increase of shrinkage with both temperature and time, evaluated at different isothermal temperatures.

As it has been explained before, to be able to calculate the parameter  $n$  from the equation (10) the isothermal shrinkage,  $\alpha$ , can be plotted with the corresponding logarithmic time as it is showed in the following figure.

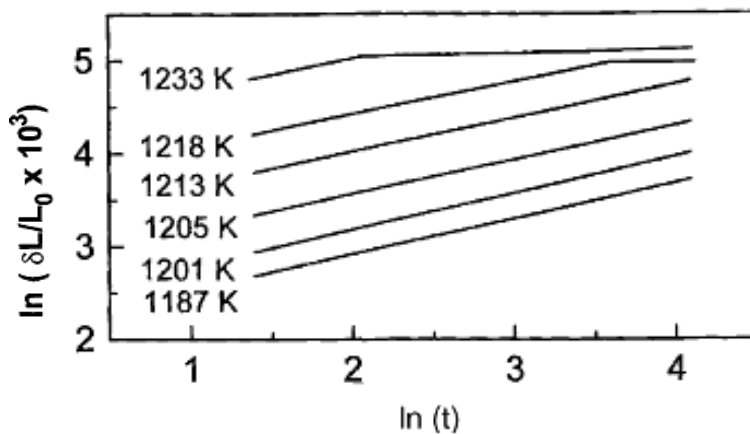


Figure 15. Example of the variation of  $\ln(\delta L/L_0 \times 10^3)$  with  $\ln(t)$  for different sintering temperatures.

With the figure above it can be observed the dependence the parameter  $n$  has with the sintering time and the sintering temperature.

#### **1.2.4 Microforming:**

The forming processes of small micro parts is not something really new for researches groups and investigations, but the challenges are present when the size/features reduce to hundreds of microns, or precision requirements for macro/miniature parts are reduced to microns. The reduction of cost for mass-manufacture of micro parts could be achieved with micro forming, but advanced technology and proper manufacturing facility must be development.

Micro-forming is recently showing a large demand due to the trend towards miniaturization. This demand comes not only for consumers, but also from technical applications. Some examples of fields where are requiring the use of miniaturization can be electronic production, micro systems technology (MST), medical sector, etc. As it is obvious, the devices related to these fields also contain mechanical parts, such as connector pins, resistor cap, screws, etc. beside electronic components, known as micro electro-mechanical systems (MEMS). The large increased in the use of MST due to the strong growth on the application fields, generates a large market for mechanical components and microparts produced in large numbers.

But as Weule et al. [53] and Westkämper et al. [54] observed, the real rupture of micro system technology was still missing. They attributed this to the fact the technologies, well understand and established in macro-manufacture, couldn't be only scale down and adapted for micro-manufacture. Different reports have demonstrated that alternative manufacturing routes can be more appropriated in order to fit the demand for economical production.

##### **1.2.4.1 Miniature manufacturing systems:**

The development on miniature manufacturing system and micro factory has attracted much attention of research groups and industries [55]. The micro parts to be produced normally are not compatible, in size, with the conventional facilities and therefore a reduction of the scale of the equipment must be taken into account. With this reduction it could be achieved a reduction of the energy consumption and materials requirements as well as of the pollution and equipment cost, etc. But more important achievement can be attributed with the reduction of the scale on the machinery and auxiliary equipment, such as an increase of the speed for the manufacturing tools, due to the dramatically decrease that could be observed on the mass of the mechanical parts. This high speed can enhance the production rates, which is one of the main targets for developers. Another significant advantage when working with miniature manufacturing systems is that the precision of the

machinery could be increased due to the fact that the force or energy loop and also the control loops are considerable short for small machinery.

But micro-manufacturing technologies are still being developed and the lack of the standardisation and knowledge as well as experience in general prevents their further applications. This is changing gradually in the last decade and nowadays some reports presented by several group of researchers can be found. They have observed that, in a micro-forming process, different effects can be described in order to understand the problems appearing currently, which also make more difficult the idea of further steps in miniaturization. Size effects are the most important factors that influence on the material behaviour, which usually occur when a reduction on the scale of the process is realized compared to the conventional size. The specimen size and microstructure influence on the flow stress, the anisotropy, the ductility and the forming limit of it.

As the process is strongly related with the material, this causes a large influence on the process [56]. The forming forces, spring-back, tribology, scatter of results and the accuracy of the samples are also additional effects that can affect the micro-forming process. These processes require high level of precision when manufacturing and therefore high precision machine tools, which availability can represent a problem, especially when manufacturing complex shapes with close tolerances and high surface quality. This required precision and also the high speed expected in this process are intrinsic problems for micro-machines and components. One obvious issue related to the mention before is the small surface the part can be supported and also its low weight, which make difficult the adhesion forces.

The measurement of micro-samples can be also a difficult procedure, which requires adequate measurement technology to be able to follow a process control and obtain the desire product quality. Another factor to take into a count might be the need to produce the parts in clean rooms, due to their extremely small dimensions. This could result expensive and maybe requires new machine concepts.

#### **1.2.4.2 Size-effect:**

If the dimensions of a forming process are scaled up or down, an effect known as size-effect occur, which make necessary the adaption of the processes as well as important the knowledge of the characteristic behaviour of the work pieces. These effects might affect to the application of the processes in a micro range and can be described as “deviations from intensive or proportional extrapolated extensive values of a process which occur, when scaling the geometrical dimensions” [57]. In general, the micro size effects refer to the surface layer model that the mechanism of forming shows and the model of material deforming when it is processed by micro forming.

Geiger et al. in 1996 divided the micro size effects into two classes: first order size effects, which can be represented by using similar sizes in similarity theory or can be explained by mean of convectional models; and second order size effects, established due to the miniaturization of the parts and cannot be represented by convectional models as the mentioned before.

Zhang et al. [58] in the other hand suggested a different classification base on the micro-forming processing system point of view: micro size effects on material constitution and micro size effects on processing condition.

- *Micro size effects on material constitution.* The evaluation of the different performances of material, under ordinary conditions, is generally realized by means of typical experiments equivalent to the complicated conditions of material forming. With these experiments, the behaviour of the deformation, under complicated conditions can be deduced. But if the forming is realized for micro size conditions, the shape and deformation behaviour of the microstructure influences more on the entire deformation behaviour of the micro part. It can be seen that the micro size effects are the reflection of the law of deformation, which in every micro size typical tests are different comparing to the one for macro forming, attributed to the change in physical, chemical or geometrical features of the material.

In addition, the micro forming related to rate as the strain rate influences, cannot be neglected on the micro size effects. It must be considered as well the high temperature properties that present the material like the case of high temperature superplastic forming.

- *Micro size effects on processing conditions.* They are represented by the qualitative property of the products, for instance the strain field and the distribution of the cross section in micro punching, and the different behaviours from those in the corresponding ordinary forming.

From the point of view of sources of size effect, following Vollertsen et al. report about size effects in manufacturing [59] these sources can be classify into two groups: physical and structural sources.

- *Physical sources.* In this group it can be done other subgroups: pure volume size (PVS) effect, surface to volume size (SVS) effect and forces relation size effect. The PVS effect is due to the decreasing volume of a part, which makes a decrease on the number of micro-structural features within that part. The reduction on the number of defects or grains makes a change eon the material behaviour, which can lead to variation on the distribution of the failure probability of the parts. The SVS effect is observed when the part size decreases and the ratio surface/volume increases, for example in heating/cooling processes this effect is generally shown. Finally, the forces relation size effect is due to other forces acting on a part

in processes, besides the processing force. These forces are usually neglected in convectional macro forming processes because they are very small, but in micro forming they should be taken into account as they result big regarding to the force used in the process. Examples of these forces can be Van-der-Waals-force, Surface tension and Gravitation.

- *Structural sources.* As in the group mentioned above, two different subgroups can be done. One, refer to the grain size to thickness size effect, which is dependent on the properties of the material and it is determined by casting condition, the mechanical, thermal and thermo-mechanical treatments. It is not possible to scale down the grain size like the part dimension as it is not possible to generate each material with each grain size. As well as the grain size, the forming processes and treatments influence the surface structure. The result is also influenced by the grain size as it has an influence on the grain inclination in forming or elastic springback in cutting operations. It results very hard to reduce the surface roughness like the part dimension. This can be attributed to the surface structure scalability, which can be seen as a source of size effects.

### **1.2.4.3 Mechanical properties:**

As mentioned above, size-effects are a very important factor to take into a count and they can strongly affect to the properties and behaviour of the material. Several researches have been reported in order to study the more appropriate method to analyse these effects and they usually mention the tensile test as the main one. But unexpected wrinkling and failure due to the eccentricity could be noticed. The Institute of Metal Forming and Casting (UTG) [60] within others worked on the development of different ideas to minimise the eccentricity as well as other methods for measuring in this field such as optical measurement system, which allows the measurement and the calculation of the distribution of the strain for a sample; or micro-laser grid in tensile test, which allow observing the local deformation and the grain size.

The size-effect also can cause a strong influence in the flow curve, which is one of the most important criteria to take into a count when designing a bulk forming processes. Decreasing the size of the sample can cause an increase in the scattering of the flow curve at room temperature. This is attributed to the decrease of the number of grains and their orientation is less averaged.

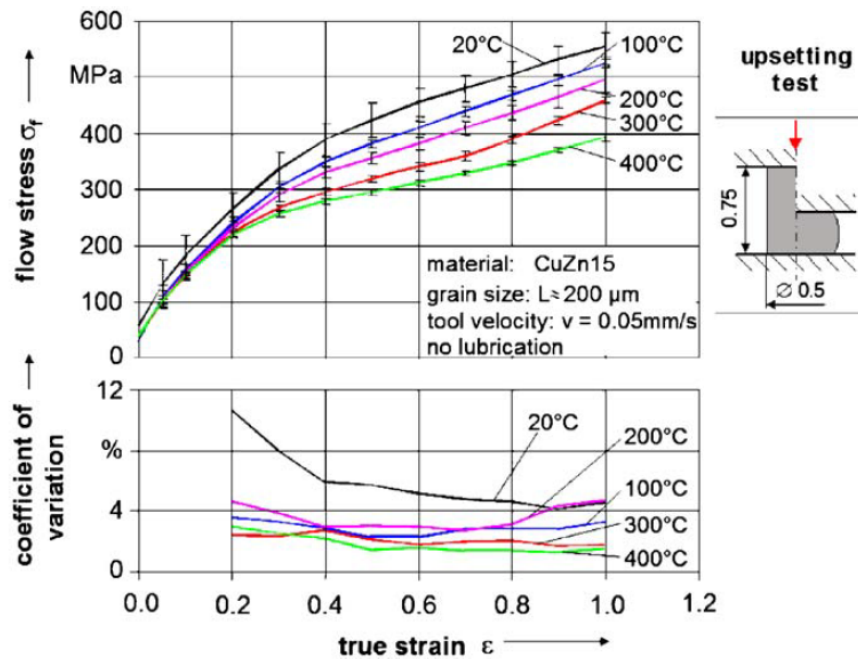


Figure 16. Example of a flow stress (above) and coefficient of variation curve (below) vs. true strain at different temperatures [61].

As it can be seen in the figure above a decrease of the flow stress can be noticed with the increase of temperature as well as it would be expected for a macro forming process. A reduction in the scatter of the flow stress when the temperature increases can be also seen in the diagram. On the diagram below it can be observed the coefficient of variation, which corresponds to the deviation of the low stress from its mean value. The large difference between the coefficient of variation at room temperature and at 400 °C, can be attributed to the individual set of grains for each sample and to the fact that at temperature, much higher than room temperature, oriented grains can be plasticised by dislocation motion mechanism.

### 1.2.5 Annealing process:

Based on the 1.1.2.2, where it was defined the structure of  $YBa_2Cu_3O_{7-x}$ ; it is known this material contains cuprates chains, which are suggested to be the reason for the reduced anisotropy in this material, comparing it to other High Temperature Superconductors. The atoms of oxygen in these cuprates chains are the most mobile and they result unoccupied sites when  $x$  decreases [62].

As it has been demonstrated in previous literature, the oxygen content found in this material, which is denoted by the factor  $(7-x)$ , affects strongly the superconducting properties [63]. It is well known that for  $0 < x < 0.6$  approximately, this material shows an orthorhombic structure, which corresponds to the superconducting phase. For values of  $x \sim 0.6$  the onset of antiferromagnetism is reached, i.e. YBCO presents a transition from orthorhombic to a tetragonal phase acting as a semiconductor material when  $x$  has a value above 0.6. An illustration of the mentioned before can be observed in the figure 17.

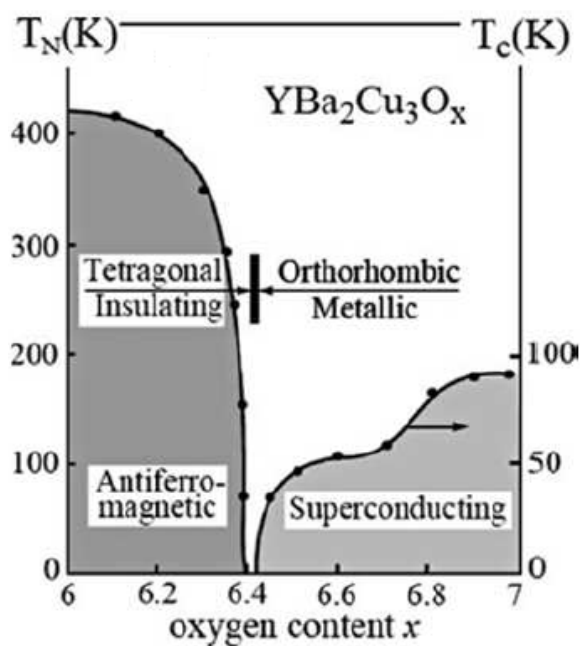


Figure 17. Phase diagram of  $\text{YBa}_2\text{Cu}_3\text{O}_x$

This value of  $x$  is the one that regulates the structural and electrical properties of the material, and when it decreases, an increased in the transition temperature,  $T_c$ , can be observed [64]. The curve, showed in figure 18, demonstrates an example of the dependence of this  $T_c$  with  $x$ , denoted by  $\delta$  in this case. When the content of oxygen is close to 7, the structure of this material is completely orthorhombic-superconductive and a high value of  $T_c$ , near 90K, can be achieved. The optimal oxygen content for this transition temperature results to be 6.87 and when it decreases from this value,  $T_c$  shows a rapid decrease.

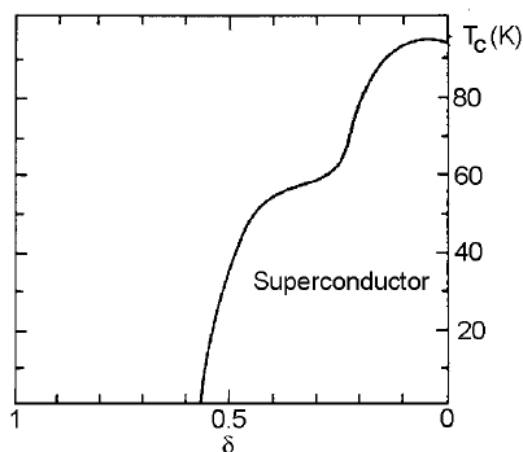


Figure 18. (Cyrot and Pavuna 1995) Example of the variation of  $T_c$  with the oxygenation in YBCO

Because all the mentioned above, an annealing under oxygen after a sintering process is necessary in order to obtain the optimum superconducting properties. This annealing process can be performed by different conditions of time, temperature and oxygen pressure. To be able to obtain the optimum parameters for the annealing process it is necessary to know the content of oxygen of the samples between other factors. The desire of analysing the quantity of oxygen content in this material has been carried out by many investigations in order to be able to obtain a correlation of this factor with any measurable parameter. Many different techniques have been used, such as coulometric titration [66], iodometric method [67], thermogravimetric analysis [68], spectrophotometric methods [69], etc. but they all result to be destructive, i.e. once it is known the characteristics of the samples, they have no more utility, and this is the main reason why became obvious the needed of non-destructive methods to evaluate the amount of oxygen in high temperature superconductors.

Ono et al. was one of the first who presented a relation between the dimension of the  $c$ -axis and the oxygen content, based on the variation of weight of annealed samples. In this case, a maximum of 6.89 of the content of oxygen was taken as a reference. Based in all the data of the cell dimensions taken from previous literatures, P. Benzi et al. found a non-destructive method in order to obtain a general mathematical relation between this content of oxygen and the cell parameters in samples of YBCO [64].

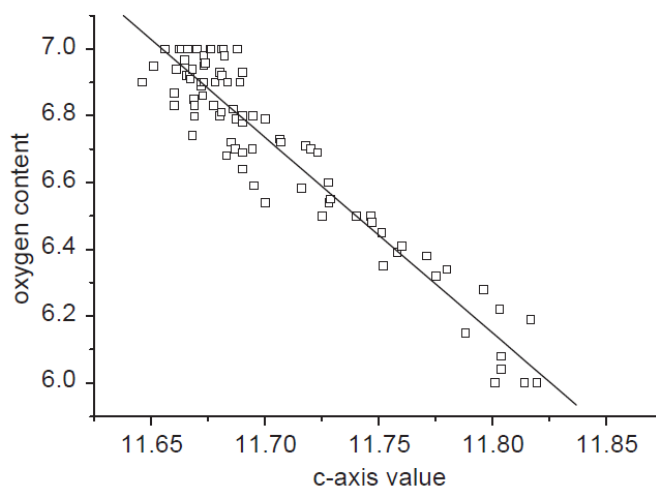


Figure 19. Value of  $(7-x)$  as a function of  $c$ -axis data from ICSD Database.

From the Database of Inorganic Crystal structure, ICSD, many structures of  $\text{YBa}_2\text{Cu}_3\text{O}_{7-x}$  were obtained and analysed plotting the values of  $(7-x)$  as a function of the values of  $c$ -axis in a graphic, as it can be seen in Figure 19. From this straight line, which defines the correlation of these two parameters, the following equation is given:

$$(11) \quad (7-x) = 75.250 - 5.856c$$

where  $c$  is the  $c$ -axis value. This equation gives consistent values for oxygen content with those obtained by iodometric titration and other techniques. Even this method can overestimates experimental results, it demonstrates that the experimental  $T_c$  are in better agreement with the content of oxygen values calculated than with the obtained from iodometric titration [58]. As this method does not involve any addition of chemical compounds and does not destroy nor damage the sample, so it allows the use of them for further applications and characterisation, it is considered a good, simple and fast way for the determination of oxygen content and for a quick preliminary analysis of the superconductive properties.

Zon Mori et al. in 2010 [70] have also studied the correlation between oxygen stoichiometry and the superconductive properties on YBCO changing the annealing time. To estimate the content of oxygen from the different values of the  $c$ -axis parameter, the equation mention above was used. In figure 3, the dependence of the content of oxygen with the time used for the annealing process is observed. It is noticed that when the annealing time increases, the value of  $c$ -axis length decreases, so the content of oxygen decreases. It is established from previous literature reviews that, for YBCO, the  $c$ -axis parameter vary from 118.4nm (for the tetragonal phase) to 116.6nm (for the orthorhombic phase) as oxygen

diffusion advances and it can be noticed that for a certain annealing time, around 12 hours, the content of oxygen remains constant. As a contrast, in the case of the transition temperature, it doesn't occur the same effect. For a certain time, the value of  $T_c$  reaches its maximum, and after this optimal time for the annealing process, it starts to decrease. This effect can be observed in the figure 21. For the case of the critical current density, an increase can be appreciated even when the transition temperature starts to decrease.

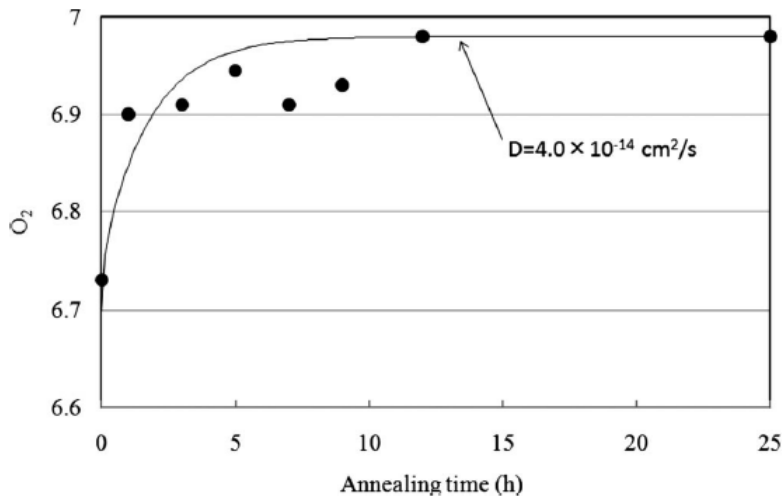


Figure 20. Dependence of annealing time with oxygen content.

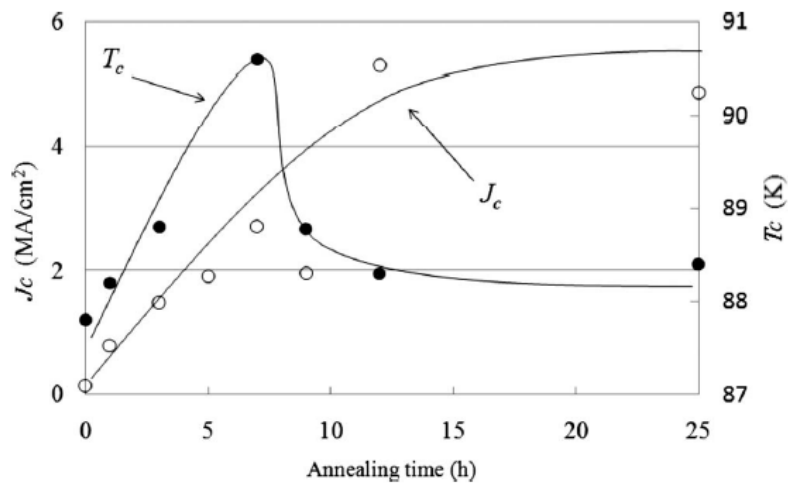


Figure 21. Variation of  $T_c$  and  $J_c$  with the annealing time

The diffusion of the oxygen along the  $c$ -axis also plays an important role to determine the optimal conditions for the annealing process. With the Crank's equation can be established the relationship between the diffusion coefficient,  $D$ , the slab thickness  $2l$  and the non-zero roots of  $\tan q_n + \alpha q_n = 0$ , where  $\alpha$  is the ratio of the number of moles of oxygen presented in the gas to the number there is in the solid [71].

$$(12) \quad \frac{M_t}{M_\infty} = 1 - \sum_{n=1}^{\infty} \frac{2\alpha(1+\alpha)}{1+\alpha+\alpha^2 q_n^2} \exp\left(\frac{-Dq_n^2 t}{l^2}\right)$$

$M_t$  corresponds to the total amount of trace present in the solid at a certain time,  $t$ , as a fraction of the amount achieved at the equilibrium,  $M_\infty$ . With the analysis carrying out by different groups of researcher, such as Akihiko Yamaji et al. has been reported that the oxygen diffusion rate in YBCO doesn't depend on the oxygen deficiency. Base on this fact, a different way to discuss the oxygen process was achieved, describing a relation between the oxygen content  $c(x,t)$  and the annealing time,  $t$ , using the following equation [64]:

$$(13) \quad \frac{\delta c(x,t)}{\delta t} = D \frac{\delta^2 c(x,t)}{\delta x^2}$$

Where  $x$  is the depth from the sample surface and  $D$ , as mentioned before, is the diffusion of oxygen, which can be determined fitting the data obtained experimentally into this equation.

To solve this equation it has been described the boundary conditions and onset conditions as the following:

- The content of oxygen on the surface is considered in equilibrium with the gases during the process of annealing and at the surface  $c(0,t)=6.89$ .
- The oxygen diffusion across the interface of the sample film/substrate doesn't occur.
- $c(x,0)$  can be used as 6.7 as an initial condition for the oxygen content as-grown sample.

Another important factor should be taken into account, when an annealing want to be performed, is the temperature and the oxygen pressure. A relation between these two factors can be observed in several research groups, such as Vazquez-Navarro et al. [72] For different content of oxygen it can be seen the dependence that the temperature has with the pressure of oxygen used for the annealing process. If this pressure is increased, higher temperature would be required for the process. The temperature most used in previous reports is around  $450^\circ\text{C}$ , which corresponds to a process using oxygen flowing at atmosphere pressure.

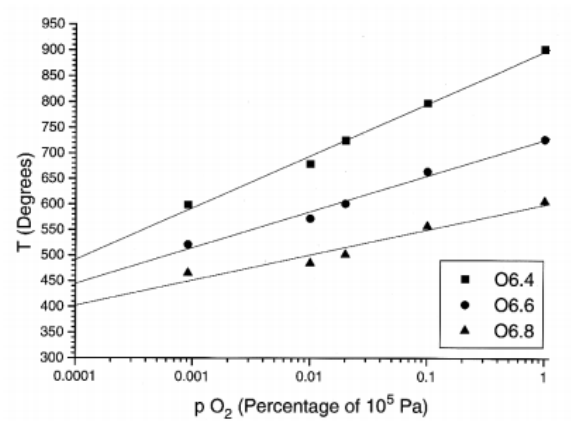


Figure 22. Vazquez-Navarro et al. prediction of equilibrium oxygenation values.

## 2. Motivation and objectives:

The study of the sintering characteristics of superconducting powders can be found in a large number of reports, as the understanding of the sintering kinetics and shrinkage behaviour of the compaction is essential for the production of single-phase and high density with crack free sintered bodies with high superconducting properties [73].

This project is presenting the study of a micro-manufacturing process. The possibility of the performance of a micro-FAST (Field Assisted Sintering Technique) is going to be study in order to obtain a full understanding of this process with a high temperature superconductor material. The work is carried out using Yttrium Barium Copper Oxide superconductor powders, most common known as YBCO or Y123, which can be easily obtained in the market. The main target of this project consists on the analysis of the procedure of a rapid-field-assisted sintering process using a Gleeble 3800 Machine and the determination of the optimal parameters to obtain high quality dense samples, so it can open the door for future improvements and investigations of the superconductivity properties for this superconductor material after a micro-FAST process. The material that is going to be used do not present any kind of dopant as many previous reports presented as the most accurate way to improve the superconductivity properties of this material. As there is no record of the use of this process with this superconductor material, it has been considered that before start working and studding different doped samples, in order to accelerate the sintering process, the optimal parameter must be established first.

The use of micro products has presented a growing demand for the last decades, not only from the point of view of consumer but also from technical applications such as medical equipment, sensor technology and optoelectronics [74]. The study of different research reports were carried out in order to understand the material deformation mechanisms and the interfacial conditions of the material as well as the properties of the micro-materials, the process modelling and analysis, the forming limits qualification and the way to optimise the process design, with a high interest on the size-effects coming from these parameters [75].

The main variables that must be taken into account in a micro-FAST are: the sintering temperature, the holding time, the heating rate and the pressure applied on the punches. To be able to perform the process, as it has been mentioned before, a Gleeble Machine will be used. In order to study the properties of the different samples it has been processed different samples varying the parameters mentioned above and using several mechanism to measure: the relative density, using a Quantix Analytical

## CHAPTER 2. MOTIVATION AND OBJECTIVES

Balance; the microstructure of the samples, using a SEM image; X-ray diffraction (XRD) will be used to be able to analyse the content of the sample so impurity phases can be identify. It can also be found images of the samples obtained after the Micro-FAST and of the micrograph from the SEM.

### 3. EXPERIMENT

#### 3.1 Micro-FAST

It has been already mention in section 1.2.4 the importance of the miniaturization of products and devices that has been developed an immense increase in the past decades. The use of microcomponents and also the competition on manufacturing cost make nowadays the cost-effective production of these components to be more important than even the quality of the final product. Different powder sintering processes have been proposed in order to apply external electric fields to assist it, such as spark plasma sintering (SPS), field activated sintering technique (FAST), pulse electric current sintering (PECS), etc.; but none of them were design to meet the needs of microforming. It was the novel microforming technology, known as Micro-FAST, which has been proposed by K. Huang et al. as a technique, which combines microforming and field-activated sintering technology for forming microcomponents using a variety of material systems [76]. Different success experiments have been carried out using this technique, such as forming of microgears [77], densification of 316 L stainless steel powder [78] and the study of the effects of heating rate and sintering temperature of this material [79], etc. It can be said that Micro-Fast is considered an efficient process as the entire forming process can be performed in a few seconds, and the relative density, obtained in the micro samples are near 100%.

In the previous experiments this research group have carried out, it has been demonstrated that the sintering parameters, the heating rate, temperature of the sintering process and the heating cycle, have a strong influence on the densification of the powder materials used for the sintering process. As Micro-FAST is a short forming process and a high pressure is continuously applied, this process occurs without experiencing a coarsening of grains [79]. In figure 1 can be observed the processed illustrated.

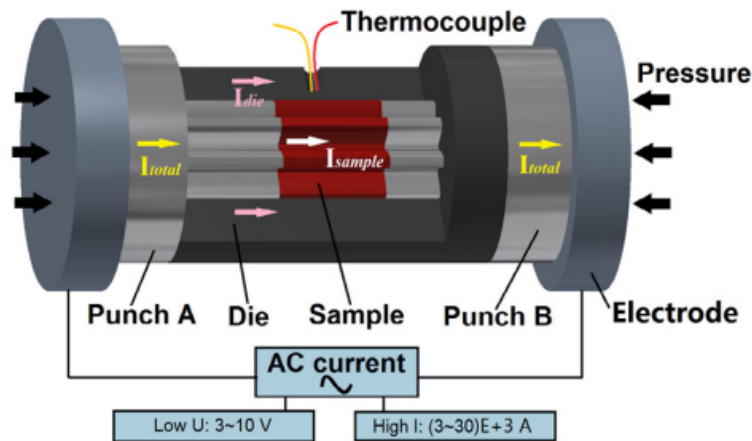


Figure 1. Modified schematic of a Micro-FAST sintering process [76]

### 3.1.1 Configuration

In order to perform a Micro-FAST process, a Gleeble 3800 was used, which characteristics can be found in section 3.2. This machine is able to generate an ac current passing through the die and the loose powders, which were poured directly inside that small die, being the die/punch set intercalated between two electrodes [77]. With this ac current it was generated the necessary temperature in the powders. The pressure onto the powders can be applied at the same time resulting easier to consolidate the powders and to achieve plastic deformation of the powders. The pressure applied can be as high as necessary, which is not possible in the case of SPS as it uses a pulsed electric current to stimulate spark discharge in gaps within the particles [80]. The pressure used in SPS is normally in a range from 15 to 50 MPa and in the case of Micro-FAST is around 100MPa.

Another important factor that makes Micro-FAST a more interesting method for sintering, compare to convectional ones is the lower sintering temperature and shorter holding time. In addition, there are more significant differences between Micro-FAST and SPS, such as higher parameters of amplitude of the electric current, which can be used up to  $10^5$  A; the pressure or the heating rate, which can be as high as  $50^\circ\text{C/s}$ . This last has not even an important influence in the final density in SPS. The time used for the sintering process is reduced in Micro-FAST, compare to other methods like SPS. In the case of Micro-FAST only a few seconds can be enough to obtain sintered samples, if the parts it is been working with are small, and it normally takes several minutes using SPS. Furthermore, Micro-FAST can restrain the grain growth and can provide

higher density and fine crystalline structure for some materials using low sintering temperature and short sintering time [77].

In conclusion, Micro-FAST is considered a promising method for sintering, as it is an energy-efficient technique, which manufacture directly from powder without binders added. This indicates it is an energy conserving method as well as environmentally friendly and impurityless forming process that allow fabricating materials with improved mechanical properties and microstructure [77].

### 3.1.2 Process

One of the most important characteristics of Micro-FAST is that it deals with miniature sizes forming components using much higher heating rates, compare to convectional sintering processes. The current density used for this project is  $>100$  kA/cm<sup>2</sup> and the material volumes involved is very small. This allows obtaining sintered samples in a very short sintering time.

The thermal curve used for Micro-FAST consists in two main steps, which happens in the same sintering process. In figure 2 can be observed an example of this thermal curve, where the first step is pointed. This first stage is fixed for all the experiment as it has been demonstrated in previous experiments, using different materials, it contains the optimum parameters to be able to release the possible gasses formed in the powders inside the die. In this first stage, the temperature is rise up from the initial temperature, correspond to the room temperature and the pressure determined for the entire process is simultaneously applied on the punch. The fixed parameters for the first stage are the following:

- Sintering temperature: 200 °C.
- First holding time: 30 s
- First heating rate: 20 °C/s
- Initial Temp. (Room Temperature): 20 °C

Using the parameters mention above, the heating time for the first stage for every process was 9 s. The material used for this project is Yttrium Barium Copper Oxide (1-2-3), with 99.5% of purity supplied by the company Alfa Aesar, which particle size is 44 µm.

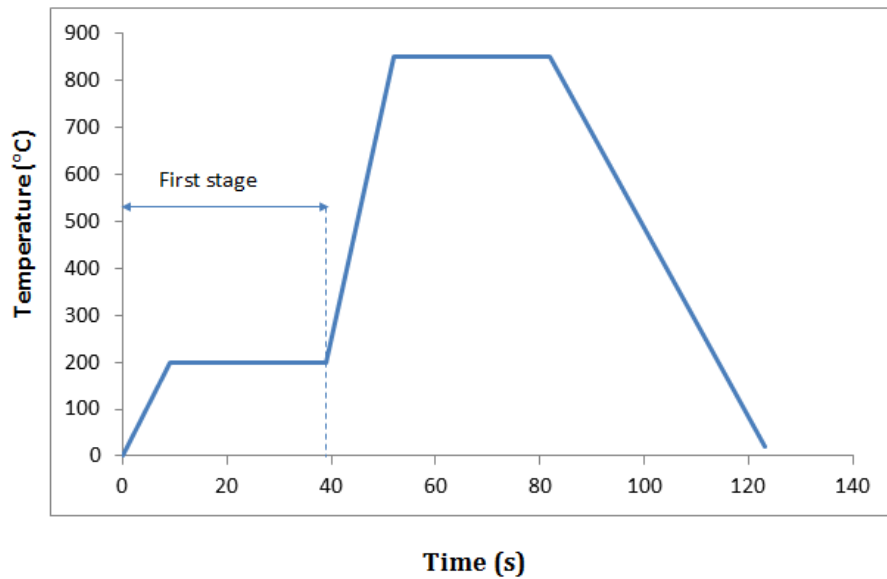


Figure 2. Scheme of thermal curve for a Micro-FAST process

For the second stage, each parameter used will be found in the next section. In this stage, the temperature goes from the first stage temperature to the sintering temperature determinate and the pressure applied on the punch is maintained. The time that this stage takes depends on the heating rate used for the process. To be able to insert in the program of the computer for the Gleeble 3800 the value of the pressure, this needed to be given in terms of the force applied to the cross section of the final sample, which correspond to the inside part of the die where the powders are situated.

$$(1) \quad Force = Pressure \cdot Area$$

To obtain the amount of powder needed for each die it was used the following equation:

$$(2) \quad mass = \rho \cdot V$$

Where  $V$  corresponds to the volume inside the die and  $\rho$  to the theoretical density of the material, in this case,  $\rho_{YBCO} = 0.006365 \text{ g/mm}^3$ .

The weight of the powders, as it has been explained before, can be calculated based on the theoretical density of the material and the volume inside the die. For these experiments, the die used was a cylindrical one, which can be seen in the figure 3. The volume of the sample obtained with this die is a cylinder as well, with a

diameter of 2mm and a height of 2mm, so the weight powder inside the die is calculated following the expression (2):

$$mass = 0.006365 \cdot \left( \pi \left( \frac{2}{2} \right)^2 \cdot 2 \right) = 0.006365 \cdot 6.2832 = 0.0400 \text{ g}$$

Based on the equation (1), the force applied with the punch on the sample during the sintering process, which is the parameter needed in the computer program for the Gleeble 3800, can be calculated:

$$Force = 125 \cdot \left( \pi \left( \frac{2}{2} \right)^2 \right) = 0.6 \text{ kN}$$

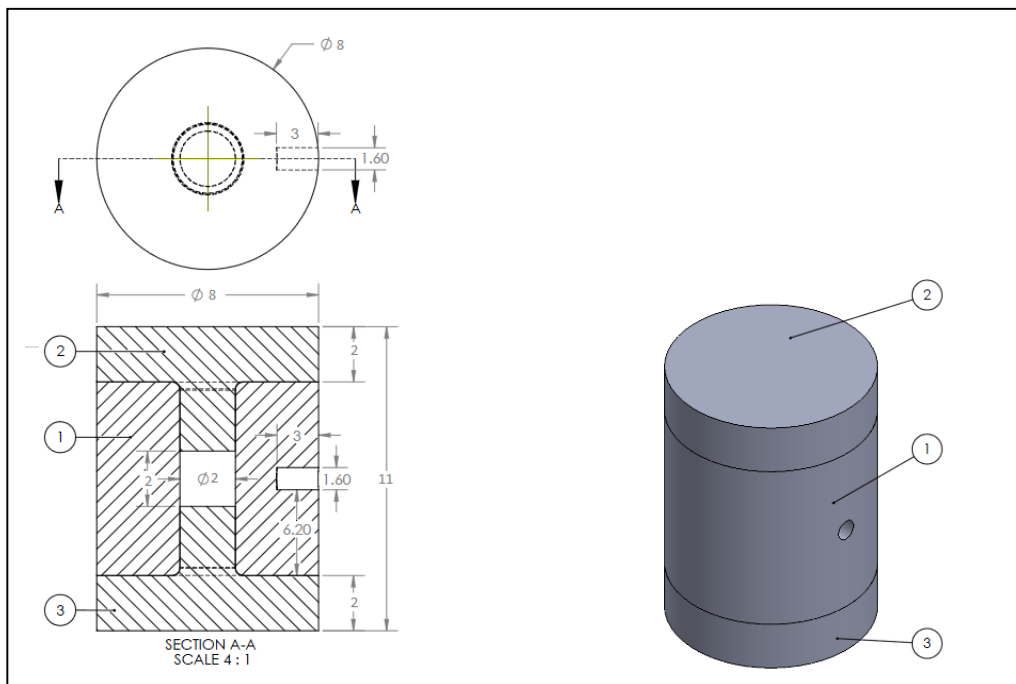


Figure 3. Die and punch assembly used for the Micro-FAST

The material used for the die and punches is graphite. This material has a high melting point, which allows to carry out experiments using sintering temperatures higher than those ones that use dies and punches made by other materials, such as tungsten carbide. Even graphite is not normally used for the punches because its low hardness, in this case it was used. The reason to use the die and the punches made by the same material is because, if they are different, they will have different thermal expansion and the retraction with each other can make the punch to get stuck into the die. Even this is taken into account, the used of an ejection was necessary in some of

the experiments to separate some of the punches from the die. Another way to improve this situation is to place a little amount of oil (fabricated with the research group for previous experiments) in the cross section of the punch in contact to the powders inside the die. This oil contains some graphite and it helps to lubricate the punch making easier to separate the die set after the sintering process.

Based on the mention above, for the following experiments several parameters are going to remain constant in the different experiments performed, as they are considered fixed for the optimum process. These fixed parameters can be observed in Table 1.

<b>Material</b>	YBCO
<b>Particle Size (<math>\mu\text{m}</math>)</b>	44
<b>Initial Temp. (Room Temp.) (<math>^{\circ}\text{C}</math>)</b>	20
<b>First Heating Rate (<math>^{\circ}\text{C}/\text{s}</math>)</b>	50
<b>First Heating Temp. (<math>^{\circ}\text{C}</math>)</b>	850
<b>First Heating Time (s)</b>	13.0
<b>First Holding Time (s)</b>	30.0
<b>Cooling Rate (<math>^{\circ}\text{C}/\text{s}</math>)</b>	20
<b>Final Tempe. (Room Temp.) (<math>^{\circ}\text{C}</math>)</b>	20
<b>Cooling Time (s)</b>	41.5
<b>Sample Radius (mm)</b>	1
<b>Sample Height (mm)</b>	2
<b>Sample Volume (<math>\text{mm}^3</math>)</b>	6.2832
<b>Theory Density (<math>\text{g}/\text{mm}^3</math>)</b>	0.006365

*Table 1. Fixed parameters for the following experiments*

### 3.1.3 Experiments

#### 3.1.4.1 Experiment No. 4-1. Parameter No. TEST

As it was the first time the Micro-FAST was going to be used to sinter superconductor powders of YBCO, we first tried with a used die with the optimum parameters we considered, based on previous experiments with different materials. The objective of this experiment was to observe if the final sample obtained after the Micro-FAST was sintered or not, i.e. if the sample still in the powders state or they presented a solid state.

<b>Weight Powder (g)</b>	0.0400
<b>Pressure (MPa)</b>	125
<b>Force (kN)</b>	0.6
<b>Second Heating Rate (°C/s)</b>	50
<b>Second Heating Temp. (°C)</b>	850
<b>Second Heating Time (s)</b>	13.0
<b>Second Holding Time (s)</b>	30.0
<b>Total Time (s)</b>	<b>123.5</b>
<b>Die Set</b>	F
<b>No. of Sample</b>	YBCO-Test
<b>Gap Between Punch &amp; Die</b>	<b>No</b>

*Table 2. Parameters used for the TEST experiment*

With the programming software this machine has install and the thermocouple placed inside the hole the die has on its side of the wall, it is possible to obtain the data of both temperatures, the theoretical one, based on the parameters we established and the real one; at each second. With the used of excel it was possible to plot this data to compare both temperatures. It has been also plot in the same graph the stroke. When the die is first filled with the powders, a gap between the two punches and the die could be seen, the stroke corresponds to the movement from this point until it reaches the complete close position of the die and punches.

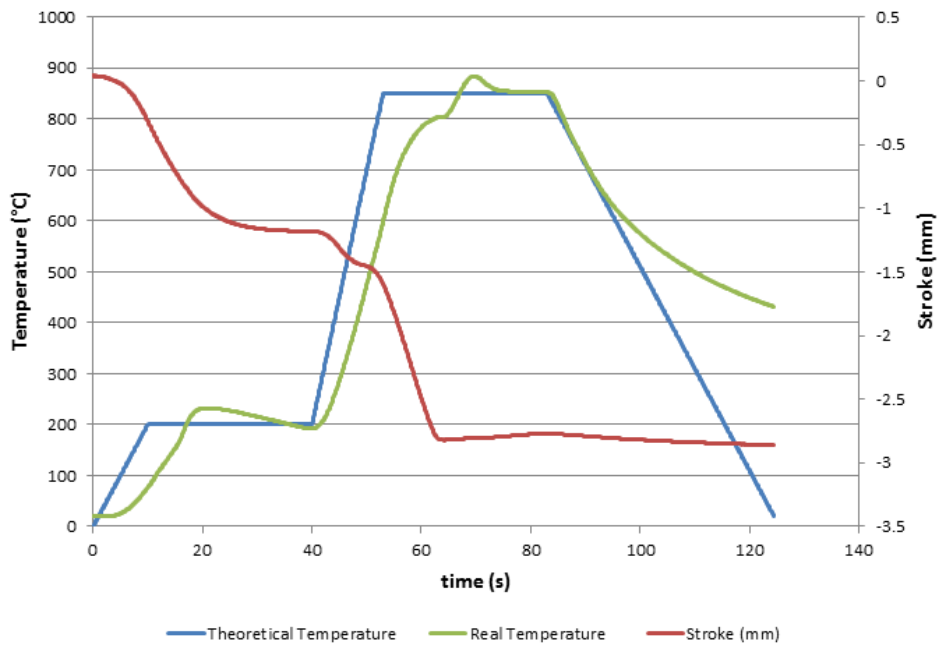


Figure 4. Graph of the experiment 4-1. Temperature and stroke vs. time.

3.1.4.2 Experiment 4-4. Parameter No. 3

Weight Powder (g)	0.0400
Pressure (MPa)	180
Force (kN)	0.6
Second Heating Rate (°C/s)	50
Second Heating Temp. (°C)	850
Second Heating Time (s)	13.0
Second Holding Time (s)	2.0
Total Time (s)	95.5
Die Set	Az1-cycle 1
No. of Sample	YBCO-3
Gap Between Punch & Die	No

Table 3. Parameters used for the experiment 4-4

For this experiment, as it can be observed in the table, the pressure and consequently the force were changed. The reason to increase the pressure from 125MPa to 180MPa was because a previous attempt with the same powder and die was performed with the pressure of 125MPa and it was observed that the temperature and heating was not transmitted to the sample, as the force was not high enough. After the increase of the force applied, the thermal curve could be obtained and the sample showed a well-sintered dense body.

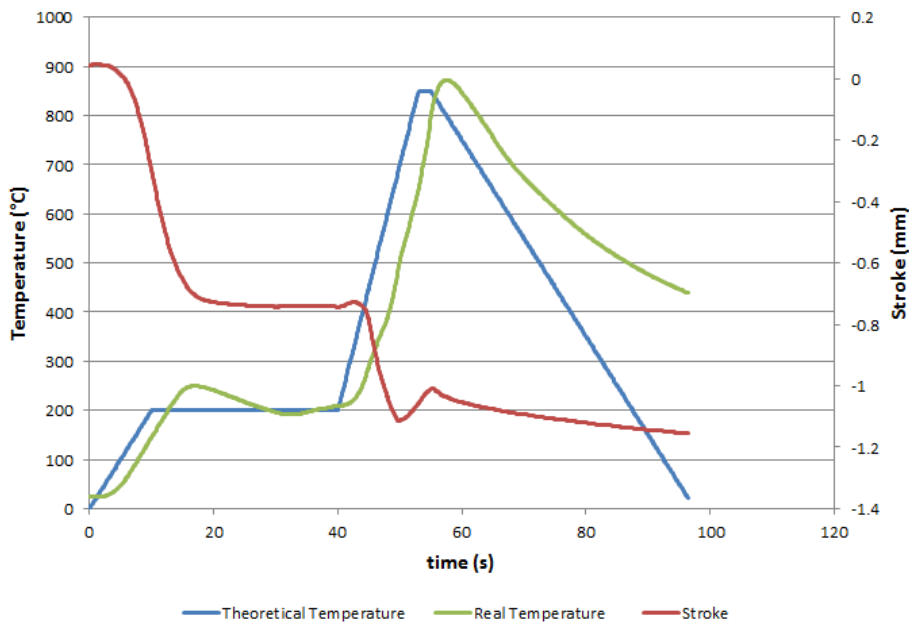


Figure 5. Graph of the experiment 4-4. Temperature and stroke vs. time.

As it can be observed, for this experiment the second holding time was changed compare to the previous one. This was realized because the main objective of this experiment is to reduce the sintering time for the entire process, so we carried out this in order to analyse experimentally the possibility of obtaining dense sample with a holding time of 2 second.

After the experiment was performed, when the die set were tried to be opened, one of the punch was broken. We think the punch didn't break during the process and we considered the process were well performed even the punch were broken afterwards. This could be attributed to the stuck of the punch inside the die, due to thermal expansion or not well lubrication.

## 3.1.4.3 Experiment 4-5. Parameter No. 4

<b>Weight Powder (g)</b>	0.0400
<b>Pressure (MPa)</b>	180
<b>Force (kN)</b>	0.6
<b>Second Heating Rate (°C/s)</b>	50
<b>Second Heating Temp. (°C)</b>	800
<b>Second Heating Time (s)</b>	12.0
<b>Second Holding Time (s)</b>	2.0
<b>Total Time (s)</b>	92
<b>Die Set</b>	A22-cycle 1
<b>No. of Sample</b>	YBCO-4
<b>Gap Between Punch &amp; Die</b>	No

*Table 4. Parameters used for the experiment 4-5*

With the experiment 4-4 we obtained a dense sintered sample, which indicates that a holding time of two second can be used for sintering process using YBCO. For this experiment 4-5 we decided to reduce the temperature as it would reduce the sintering time for the process and also could give us different properties of the sample in order to analyse the results of them afterwards and study the influence of the temperature in the microstructure and relative density. In this case, as in the previous experiment, one of the punches was broken after trying to separate it from the die.

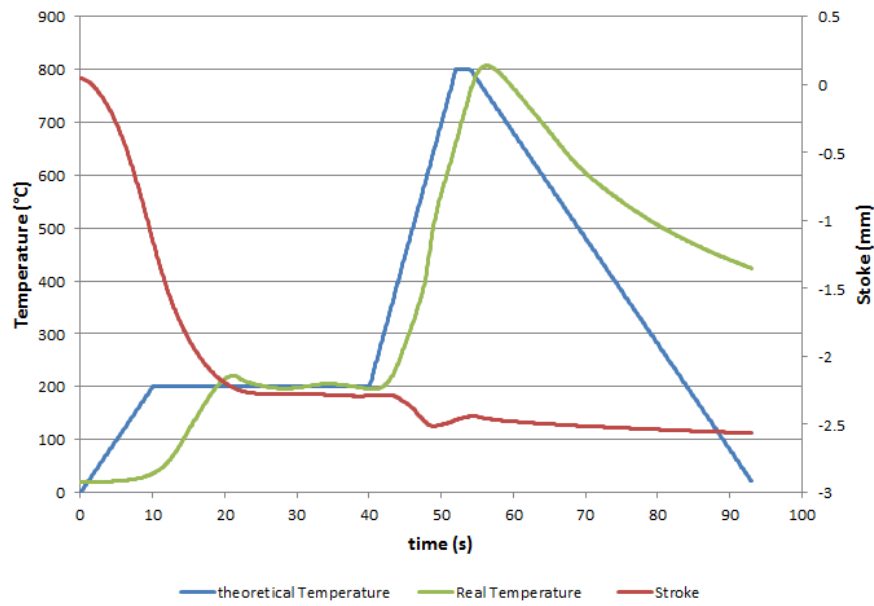


Figure 6. Graph of the experiment 4-5. Temperature and stroke vs. time.

#### 3.1.4.4 Experiment 4-26. Parameter No. 5

For this experiment, we decided to perform the process with a temperature 50°C under the one used in the previous experiment as it would reduce the sintering time to 88.5 seconds. The punches after this experiment could be removed from the die easily, this can be due to the fact that the temperature used in this case does not cause a high thermal expansion.

Weight Powder (g)	0.0400
Pressure (MPa)	180
Force (kN)	0.6
Second Heating Rate (°C/s)	50
Second Heating Temp. (°C)	750
Second Heating Time (s)	11.0
Second Holding Time (s)	2.0
Total Time (s)	88.5
Die Set	A27-cycle 1
No. of Sample	YBCO-5
Gap Between Punch & Die	No

Table 5. Parameters used for the experiment 4-6

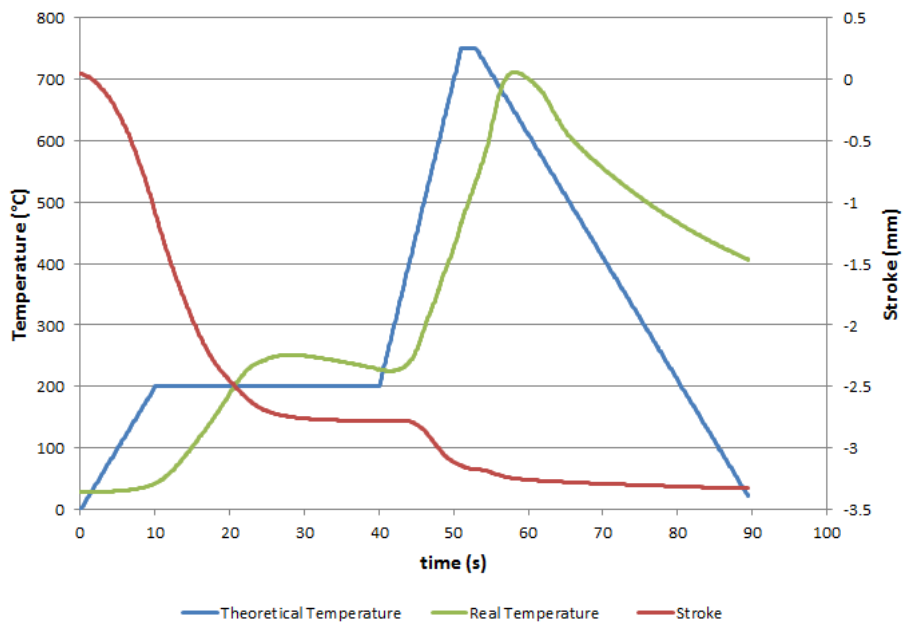


Figure 7. Graph of the experiment 4-6. Temperature and stroke vs. time.

**3.1.4.5 Experiment 4-27. Parameter No. 6**

For this last experiment a change in the temperature was carried out. Unlike the previous ones, the temperature for this case was increased until 900°C. The reason for using a higher temperature is because after several hours, the sample obtained from the experiment 4-26 was broken; indicating that the density of the sample must not be near the theoretical density of this material and this can be attributed to the low temperature used in this experiment.

<b>Weight Powder (g)</b>	0.0400
<b>Pressure (MPa)</b>	180
<b>Force (kN)</b>	0.6
<b>Second Heating Rate (°C/s)</b>	50
<b>Second Heating Temp. (°C)</b>	900
<b>Second Heating Time (s)</b>	14.0
<b>Second Holding Time (s)</b>	2.0
<b>Total Time (s)</b>	99.0
<b>Die Set</b>	A26-cycle 2
<b>No. of Sample</b>	YBCO-6
<b>Gap Between Punch &amp; Die</b>	No

*Table 6. Parameters used for the experiment 4-7*

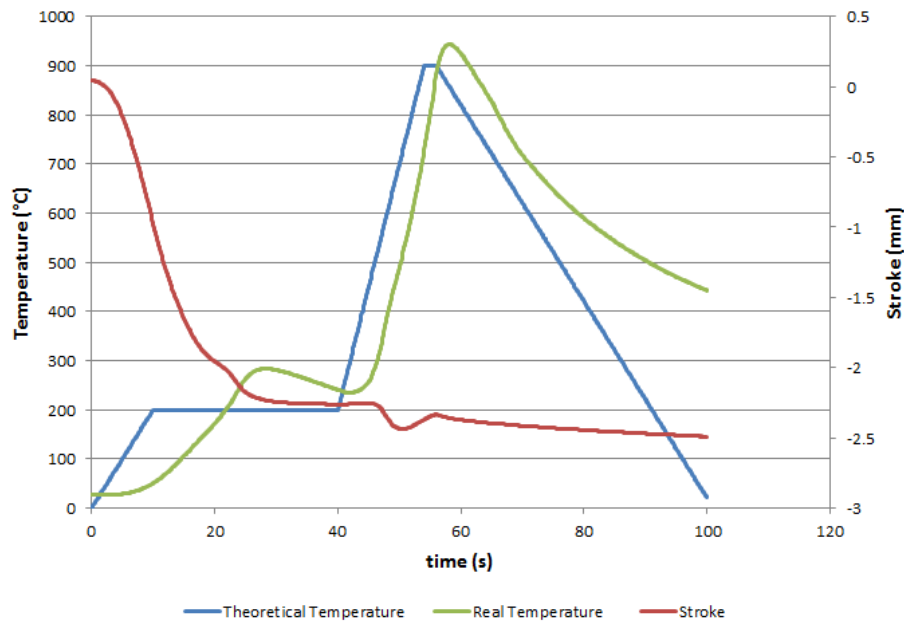


Figure 8. Graph of the experiment 4-7. Temperature and stroke vs. time.

As it can be observed in all the graphs shown above, the curve corresponded to the real temperature follow the one describe by the theoretical one but some differences can be observed. The sintering temperature reached in all the cases is higher than the determined and the holding time, especially for the samples YBCO-5 and YBCO-6, result smaller than the one introduced in the computer.

It can also be pointed out that the stroke remains constants before the second stage of the sintering process in all the experiments but in the case of the Test-1 and the YBCO-3. The first one can be attributed to the fact that the die and punches had been used before this experiment, so maybe they suffered an expansion in the previous experiments they were used, making the movement of these parts more difficult for our experiment. In the case of the sample YBCO-3, this experiment was performed before with a pressure of 125MPa and after observing the temperature was not being transmitted, the pressure was increased to 180 MPa. This previous attempt could make the die and punches expand a little bit making more difficult the movement of them in the experiment.

## 3.2 Gleeble Machine

### 3.2.1 The monitoring and programming

The Gleeble 3800 can be operated by computer, by manual control, or by a combination of both. The computer control consists of a Windows based computer with a programming software, in this case *QuickSim*, where the different parameters that defined the sintering process can be established and which allows arbitrary programming of waveforms for both thermal and mechanical systems. These parameters, described by the thermal cycle and time displacement curve in previous section can be changed for each experiment and they would be the theoretical parameters that the machine will follow. The Windows program offers a flexible industry standard multi-tasking Graphical User Interface, which allows to create simulation programs and to analyse the results in order to perform reports and presentations.

In figure 9 it can be observed the digital control system of the Gleeble 3800, which provides the necessary signals to control thermal and mechanical test parameters simultaneously through the digital closed loop servo systems. In this display it can be seen the theoretical data established in the computer and the real parameters the sample is suffering. To be able to measure the real temperature, a pair of thin thermocouples were attached to each other and placed into a small hole situated in one side of the die, where the end of the cable of the thermocouple fit perfectly so it does not move during the entire process. The other sides of the thermocouples were connected to the machine as it can be observed in figure 10.



Figure 9. Real-time parameter display on console computer

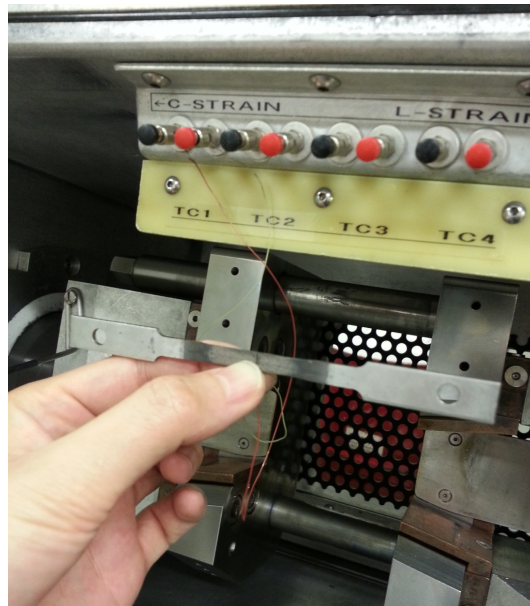


*Figure 10. Connection of the thermocouples.*

### **3.2.2 Mechanical**

The basic mechanical set up of the Gleeble machine contains two different sides, which can be considered symmetrical; this can be observed in figure 11. A hydraulic cylinder drives one of the sides, the left one, however the right side is a fixed jaw. In order to place the specimen fixture, the machine provides slots on both sides. To adjust the die in between the two sides, the manual option was used in order to apply the minimum pressure needed to situate the die so it does not fall.

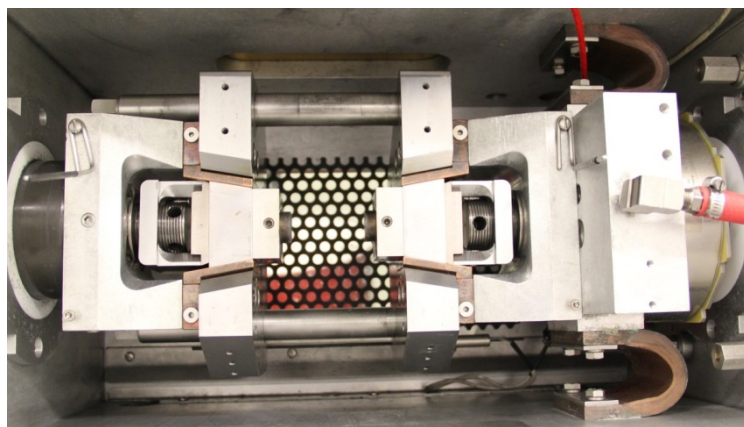


*Figure 11. Block and wedges placed into the machine*

Gleeble 3800 offers a high-speed mechanical system with unmatched performance. Following the system specifications of this machine it can be observed that the latest in state-of-art high speed servo-hydraulic valves combined with innovative hydraulic system design create a high speed servo system, which is capable of two meters per second. It allows independent control and programming of the strain and of the strain rate, which are only found on Gleeble systems.

This tooling set is placed in a chamber, which can be tightly closed in order to obtain a vacuum chamber. The dimensions of the rectangular chamber where the process is taking place is  $l=525\text{mm}$ ,  $h=290\text{mm}$  and  $t=400\text{mm}$ , where  $l$  correspond to the length of the chamber,  $h$  to the height and  $t$  to the thickness, i.e. from the outside of the chamber to the inside. The time needed to obtain the vacuum atmosphere depends on the degree of the vacuum required for the experiment. For the experiment carried out the usually level applied is  $4.5 \times 10^{-1}$  Torr (1 Torr is equal to 1 mmHg) and this normally took around 3 or 4 minutes.

### 3.2.3 General specifications of the mechanical system

From the specific manual of the Gleeble 3800 it can be collected the maximum and minimum value of the most important parameters the machine can stand, such as the force in compression and in tension, the stroke rate and distance, and the measurement of the accuracy and resolution of the force, stroke and also of the C-strain. The values of these parameters are collected in the following table

Test Frame	Horizontal type with dual 99mm diameter columns (3.9 inches)
Mechanical system	Closed-loop hydraulic servo control
Maximum force/load in compression	20,000 kg (~44,000 lbs.) (196 kN)
Maximum force/load in tension	10,000 kg (~22,000 lbs.) (98 kN)
Maximum stroke rate	2,000 mm/s in tension or compression
Minimum stroke rate	0.001 mm/s in tension or compression
Maximum stroke distance	125 mm*
Maximum number of compression strokes	10 strokes (hits) over 20 mm distance
Force measurement accuracy	$\pm 1.0\%$ of full scale
Stroke measurement accuracy	$\pm 0.5\%$ of full scale
C-strain measurement accuracy	$\pm 0.5\%$ of full scale
Force measurement resolution	$\pm 1$ kg
Stroke measurement resolution	0.002 mm
C-strain measurement resolution	0.002 mm

*Table 7. General specification of mechanical system from the manual of Gleeble 3800*

[81]

Accuracy conditions are at room temperature of 23°C and the maximum stroke rates are at hydraulic pressure of 211 kg/cm<sup>2</sup> and oil temperature of 40°C.

\*May be limited by certain jaw configurations

### 3.2.4 Electrical and thermal properties

The electric connections of each part and tool can be observed in figure 11, where it is represent with blue arrows the electric current flow. The current pass through the grips and the samples as there is no insulation material to prevent electrical pass or heat transfer.

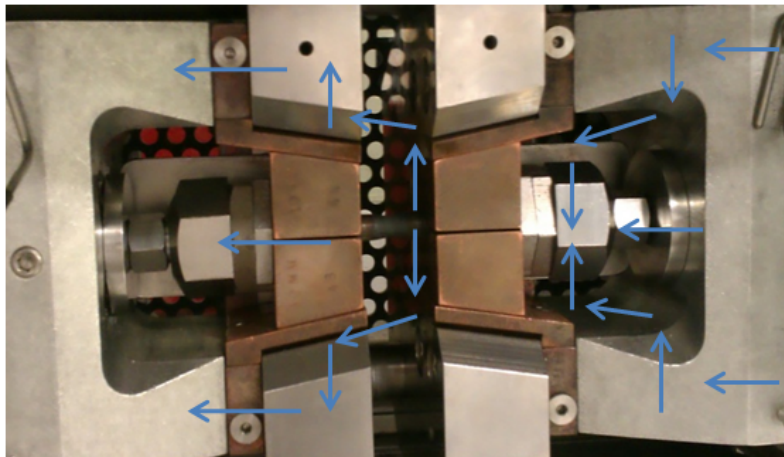


*Figure 11. Electric current flow on the parts and tool inside the machine*

The thermal system using in the process is the ISO-T Flow stress Compression Testing, which anvil base can be observed in the figure above. This flow stress compression anvils provide a uniform distribution of the temperature throughout the compression specimen during the single and multiple deformation tests.

Another important facility of this machine is the cooling system. The Gleeble 3800 contains two cooling systems. One of them is the system/process cooling, which uses water running constantly during the machine operation process and helps to avoid a possible overheat in the machine. This system is supply by KoolantKoolers. The other cooling system is the specimen cooling/quenching, which uses air or water to cool down the specimen rapidly. The maximum value for quenching is 10000 °C/s, which is lower than the value needed for this experiment.

## 4. ANALYSIS AND RESULTS

In this last section it will be described the different analysis performed to the samples obtained from the sintering process Micro-FAST, described in the previous section. As it can be observed, five samples can be studied, which four of them present a dense body fabricated from powders of YBCO. A brief explanation of the machines used for the analysis and the reasons to carry out them can be also found.

### 4.1 Relative Density

The density of the samples has been calculated using a Practum analytical balance with a density kit. This machine allows us to determine the density of the samples by means of Archimedes' principle, which states that a body immersed in a fluid can be said it loses weight by an amount equal to the weight of the fluid it displaces [82].



*Figure 1. Practum analytical weight balance*

Once the value of the density of each sample is known with this device, the following formula is used in order to calculate the relative density, according to the theoretical value of the density.

$$(1) \rho_r = \frac{\rho}{\rho_o}$$

where  $\rho_r$  is the relative density,  $\rho$  the density calculate with the weight balance and  $\rho_o$  the theoretical value.

**YBCO-TEST-1**

The four main parameters used for this experiment were:

- Sintering temperature: 850 °C
- Pressure: 125 MPa
- Second holding time: 30 s
- Second heating rate: 50 °C/s

Sample name	Parameter	1	2	3	Average
YBCO-TEST-1	Mass (g)	0.0365	0.0365	0.0365	0.0365
	Density (g/cm <sup>3</sup> )	4.99	4.43	5.358	4.926

Table 1. Density measurements of the sample Test-1

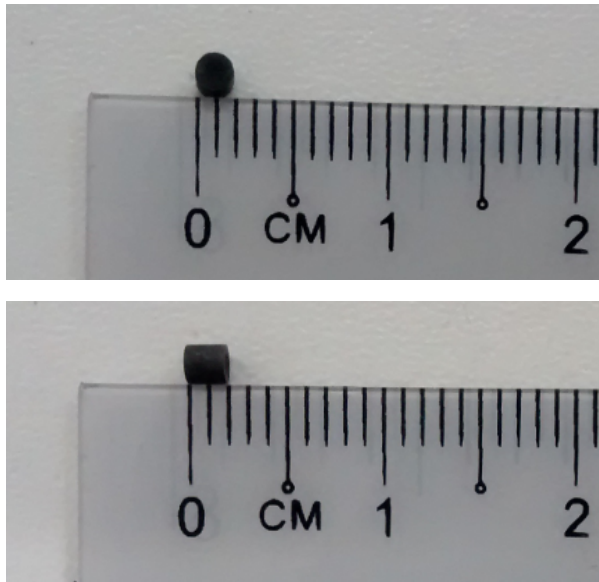


Figure 2. Optical view of the dimension of the sintered sample Test-1

$$\rho_r = \frac{4.926}{6.365} = 0.774$$

Which indicates a value of **77.4%** of the theoretical density.

**YBCO-3**

The four main parameters used for this experiment were:

- Sintering temperature: 850 °C
- Pressure: 180 MPa
- Second holding time: 2 s
- Second heating rate: 50 °C/s

Sample name	Parameter	1	2	3	Average
YBCO-3	Mass (g)	0.0325	0.0326	0.0327	0.0326
	Density (g/cm <sup>3</sup> )	3.461	4.504	4.519	4.161

Table 2. Density measurements of the sample YBCO-3

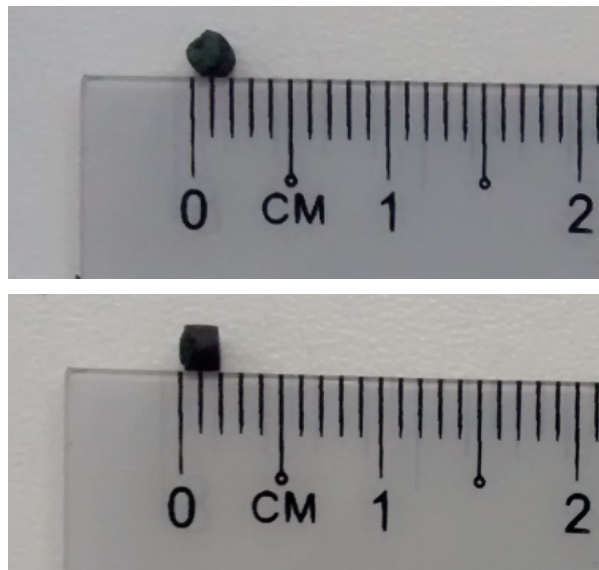


Figure3. Optical view of the dimension of the sintered sample YBCO-3

$$\rho_r = \frac{4.161}{6.365} = 0.654$$

Which indicates a value of **65.4%** of the theoretical density.

#### **YBCO-4**

- Sintering temperature: 800 °C
- Pressure: 180 MPa
- Second holding time: 2 s
- Second heating rate: 50 °C/s

The relative density of this sample could not be measured as the sample was found broken in three pieces several hours, after the sintering process was carried out. An image of it can be observed below as a proof of this. The reason of this could be attributed to a low density of the sample obtained.



*Figure 4. Optical view of the dimension of the sintered sample YBCO-4*

#### **YBCO-5**

- Sintering temperature: 850 °C
- Pressure: 180 MPa
- Second holding time: 2 s
- Second heating rate: 50 °C/s

Sample name	Parameter	1	2	3	Average
YBCO-5	Mass (g)	0.0390	0.0395	0.0394	0.0393
	Density (g/cm <sup>3</sup> )	4.747	4.915	5.042	4.901

Table 3. Density measurements of the sample YBCO-5

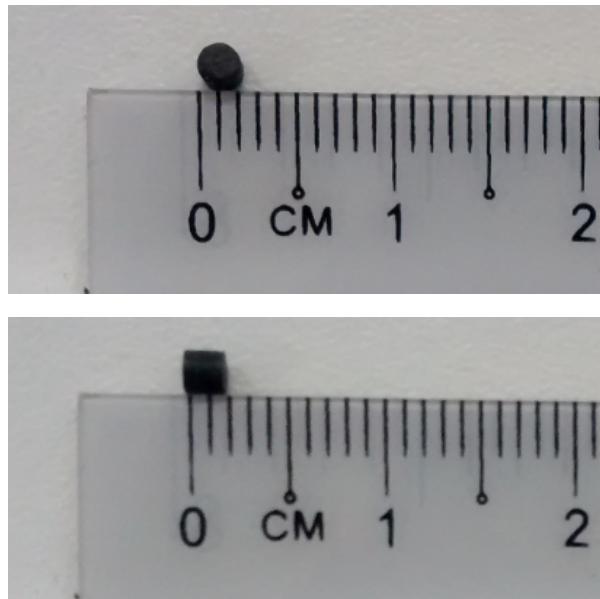


Figure 5. Optical view of the dimension of the sintered sample YBCO-5

$$\rho_r = \frac{4.901}{6.365} = 0.770$$

Which indicates a value of **77.0%** of the theoretical density.

**YBCO-6**

- Sintering temperature: 900 °C
- Pressure: 180 MPa
- Second holding time: 2 s
- Second heating rate: 50 °C/s

Sample name	Parameter	1	2	3	Average
YBCO-6	Mass (g)	0.0374	0.0378	0.0379	0.0377
	Density (g/cm <sup>3</sup> )	4.497	4.836	4.503	4.612

Table 4. Density measurements of the sample YBCO-6

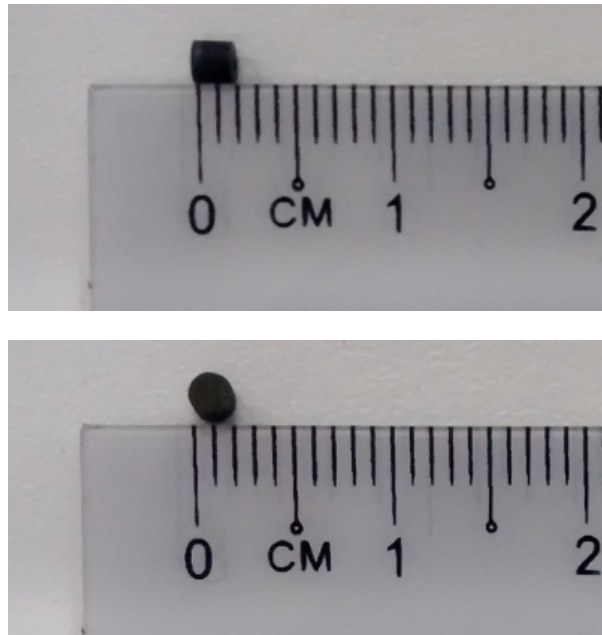


Figure 6. Optical view of the dimension of the sintered sample YBCO-6

$$\rho_r = \frac{4.612}{6.365} = 0.725$$

Which indicates a value of **72.5%** of the theoretical density.

The relative density of all of the samples is under the 80%, which is not a good result as the material can provide weak mechanical properties with this low density, but it is needed to take into account that these samples, as it has been mentioned before, need an annealing in oxygen after the sintering process, being able to increase the relative density up to values of 90%. In figure 7 can be observed the change of the relative density with the annealing time shows a linear dependence.

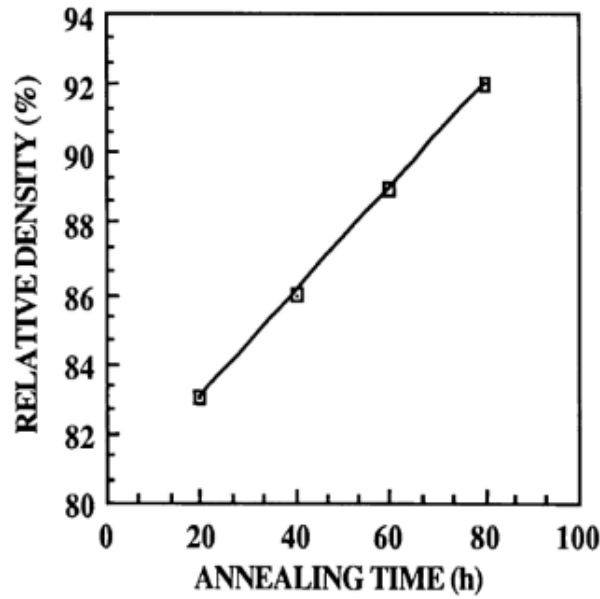


Figure 7. Example of the variation of the relative density of a sample of YBCO with the annealing time at a certain temperature [1]

#### 4.2 X-Ray diffraction study

The studies with X-ray are normally used for analysis of the crystal structure, which is very important for the understanding of physical properties and defining guidelines to be able to explore new materials. The different chemical elements that are present in HTS oxides, beside copper and oxygen, can be observed and show common structure features, such as pronounced layer character. X-ray diffraction is considered one of the most important experimental techniques to reveal crystal structure, which can provide information about detailed constitution of the material, i.e. element substitutions, thermal motion, interatomic distances, the nearest neighbour atomic environments [83].

By means of scattering and absorption, X-rays interact nearly exclusively with the material's electrons. The theory developed by W. L. Bragg, which states that the lattice planes can reflect radiation as a mirror, is one of the most powerful principles in the diffraction theory. It is observed that the positive maximum interference happens when the differences in the path among reflections from successive lattice planes of the same family is equal to an integer number of wavelength

$$(1) \quad n\lambda = 2d \cdot \sin \theta$$

Where  $n$  corresponds to the order of reflection,  $\lambda$  to the wavelength,  $d$  to the lattice plane spacing and  $\theta$  to the angle of incidence or reflection to the planes. To every family of lattice planes parallel, can be associated a point in reciprocal space, which form a periodic lattice when they are all together. In order to occur the diffraction, a reciprocal lattice, defined by the vector  $d_{hkl}^*$ , is found on the surface of Ewald sphere. This sphere is observed in figure 8, and it has a radius of  $1/\lambda$ . The lattice points are able to diffract if they are placed inside the sphere of radius  $2/\lambda$ . The wavelengths used for these diffraction experiments must have a magnitude equal to the interplanar distances in crystal [83]

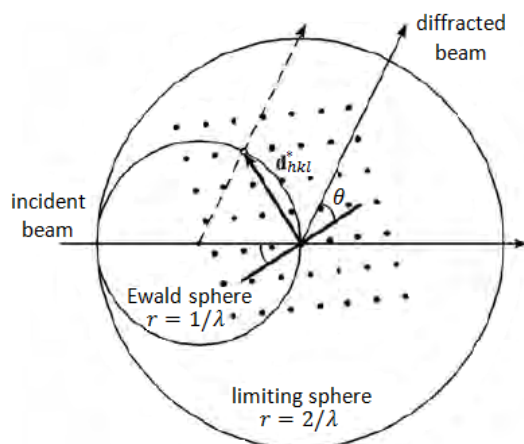


Figure 8. Diffraction of X-ray by a single crystal

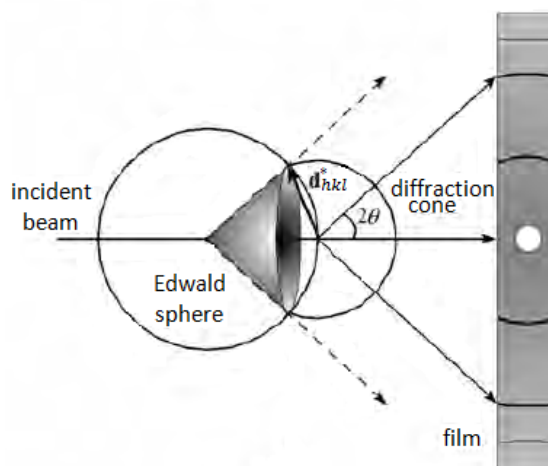
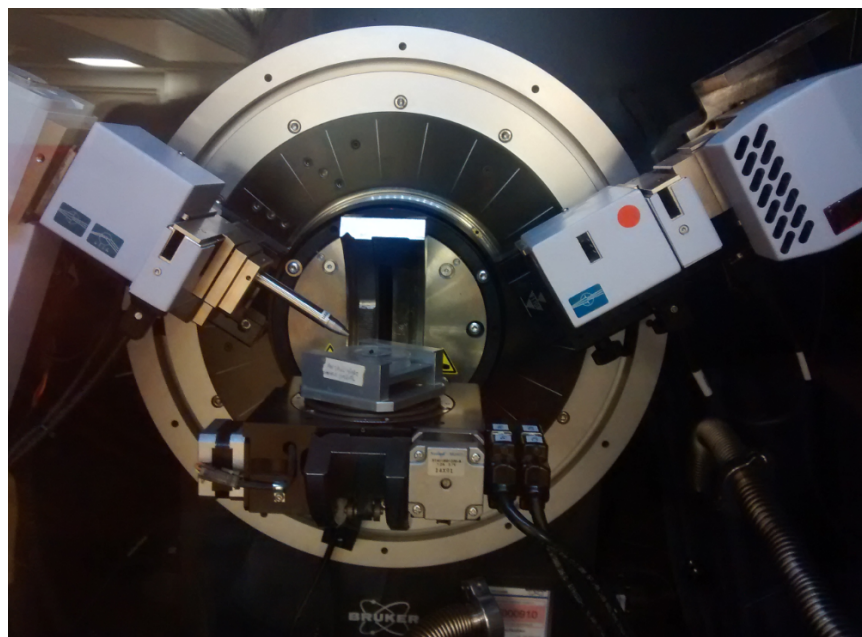


Figure 9. Diffraction of X-ray by a single crystal (top) and Diffraction of X-rays by a powder (bottom)

For HTS cuprates, the crystal structures are generally defined as a stacking of atom layers and they are usually grouped into several structure series [83]. In the case of  $YBa_2Cu_3O_7$ , the undistorted structures correspond to the orthorhombic, this is because the presence of additional CuO layers with O atoms, which are placed in the centre of the square edges in one direction only. The theory of the structure of YBCO can be found in section 1.1.2.2. Small displacements of the atoms, an ordered arrangement of cations between layers of the same type and of vacancies or even the insertion of extra atoms can be the reason for a reduction of the tetragonal symmetry, which is normally observed in the real structure. These lead to orthorhombic structures in the majority of the cases. The cell vectors found along the diagonals of the tetragonal cell base of an ideal structure are  $a + b$ ,  $-a + b$  and  $c$  [83].

For the samples obtained after the Micro-FAST experiment, an X-ray study was ready to be performed at the laboratory of Strathclyde with the machine D8 Advance, which is shown in figure 10. With this X-ray analysis it is possible to calculate the lattice parameters, and an estimation of the content of oxygen can be carried out if the dimension of the c-axis is known so the time needed for the annealing process subsequently the sintering process can be acquired.



*Figure 10. D8 Advance Bruker machine to perform the XRD.*

The data from this analysis was not possible to be obtained, as the dimension of the samples was not big enough to be noticed by the machine and show the peak in

the graph, which represent the c-axis. The parameters used for this attempt was a  $2\theta$ -range from  $10^\circ$  to  $70^\circ$  in the  $2\theta$ - $\theta$  scan mode with 0.02 steps.

### 4.3 Scanning Electron Microscopy (SEM)

The scanning electron microscope is a standard analytical device, which allows the study of a large range of materials. The most used function of this tool is to analysis surface features and topography with images at magnifications up to 100,00. For our samples it will be used to identify the microstructural features, such as homogeneity, porosity, roughness and/or connectivity.

In addition, the device is fitted with energy dispersive X-ray detector (EDX), which allows performing aspatially resolved elemental analysis. It provides information of the elements content in a certain region of the sample.

The following images correspond to the SEM and EDX for the different samples obtained in our experiment after performing a Micro-FAST. As it can be observed the first image of the samples are without any magnification, so the hole body can be showed and the other two images has been taken of the centre of the sample and one of the side, both with a magnification of 1500.

The SEM has been performed in the surface of the samples because, to be able to analyse the inside of them, they needed to be cut in two pieces and this would make the sample not able for future use or analysis. In addition, the samples result to small to assure a success of this procedure, being difficult to break them.

4.3.1 YBCO-Test-1

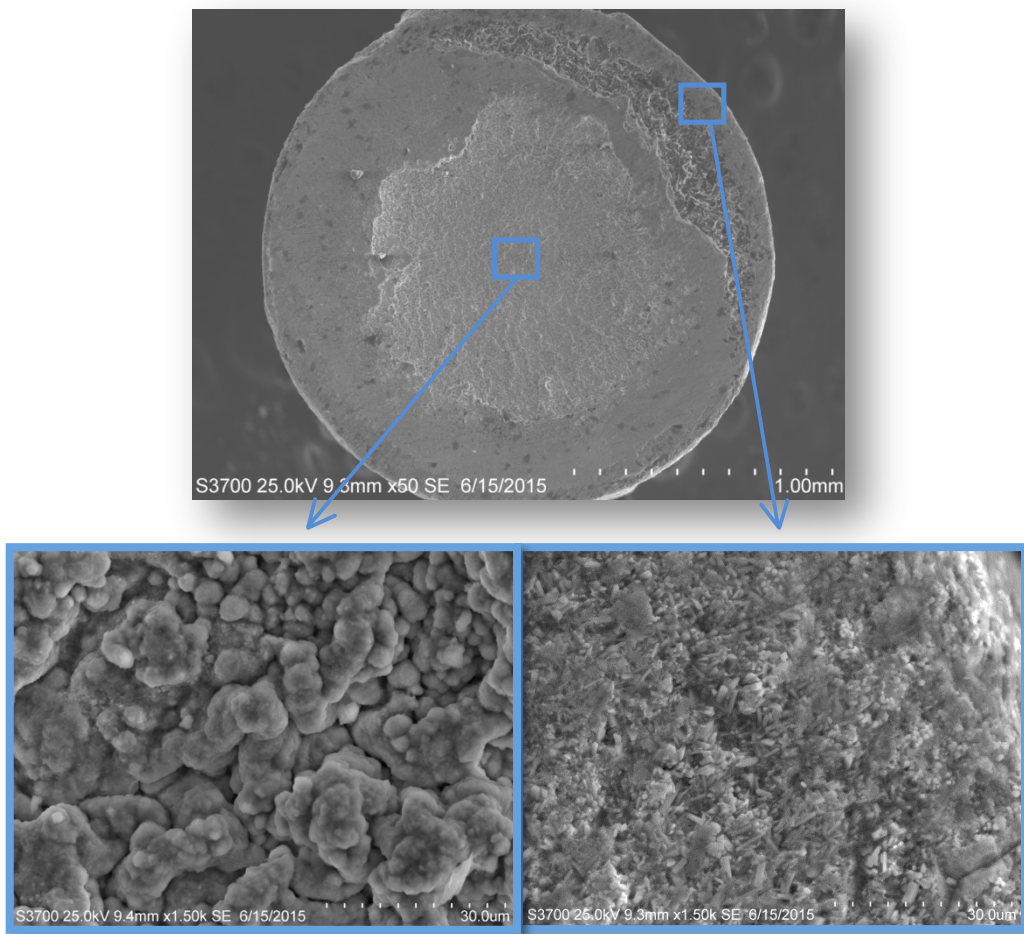


*Figure 11. SEM micrograph of the sample YBCO-Test-1 sintered at 850 °C and 30 seconds of holding time in the second stage.*

As it can be observed in this sample, the densification has been obtained from powder raw material, as it can be seen the formation of chains from these powders, which are connected between each other forming a dense bulk. The main difference between the image from the centre and the image of one of the side is due to the content of C found on that side of the sample. This content of carbon is attribute to the reaction between the YBCO and the graphite of the die and punch.

4.3.2 YBCO-3

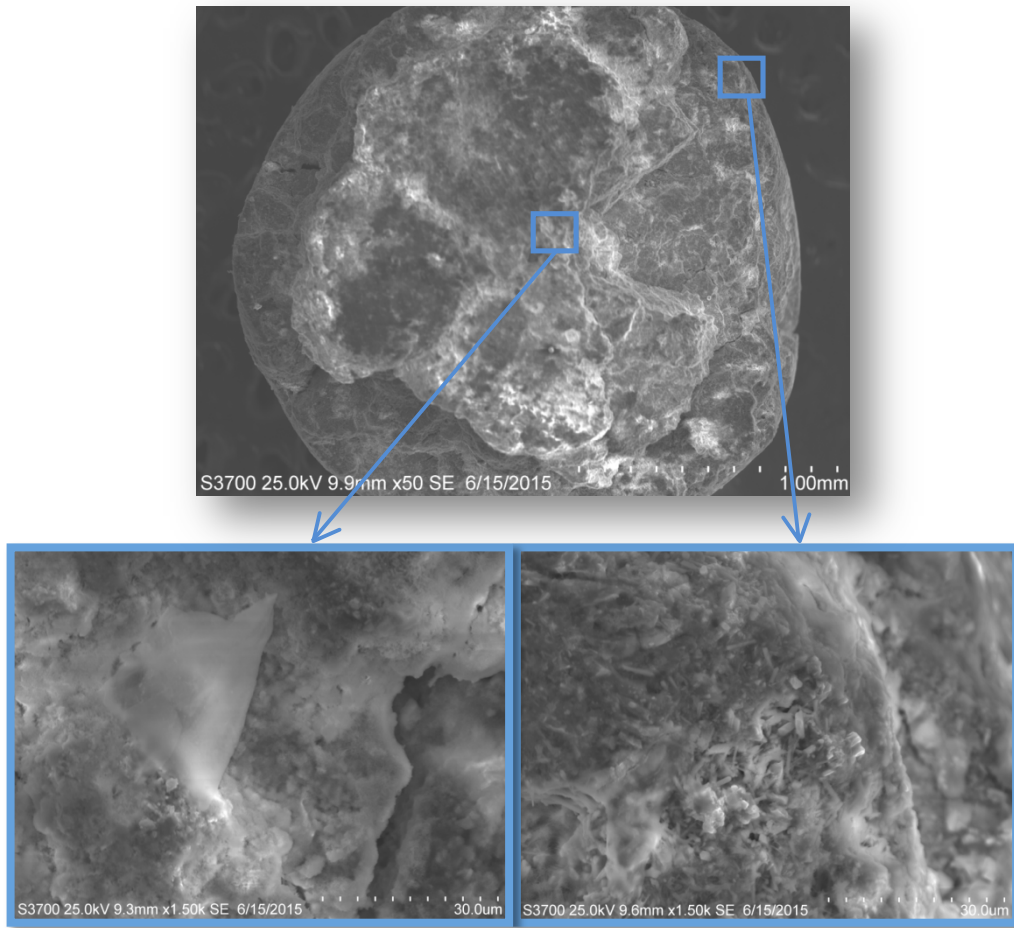
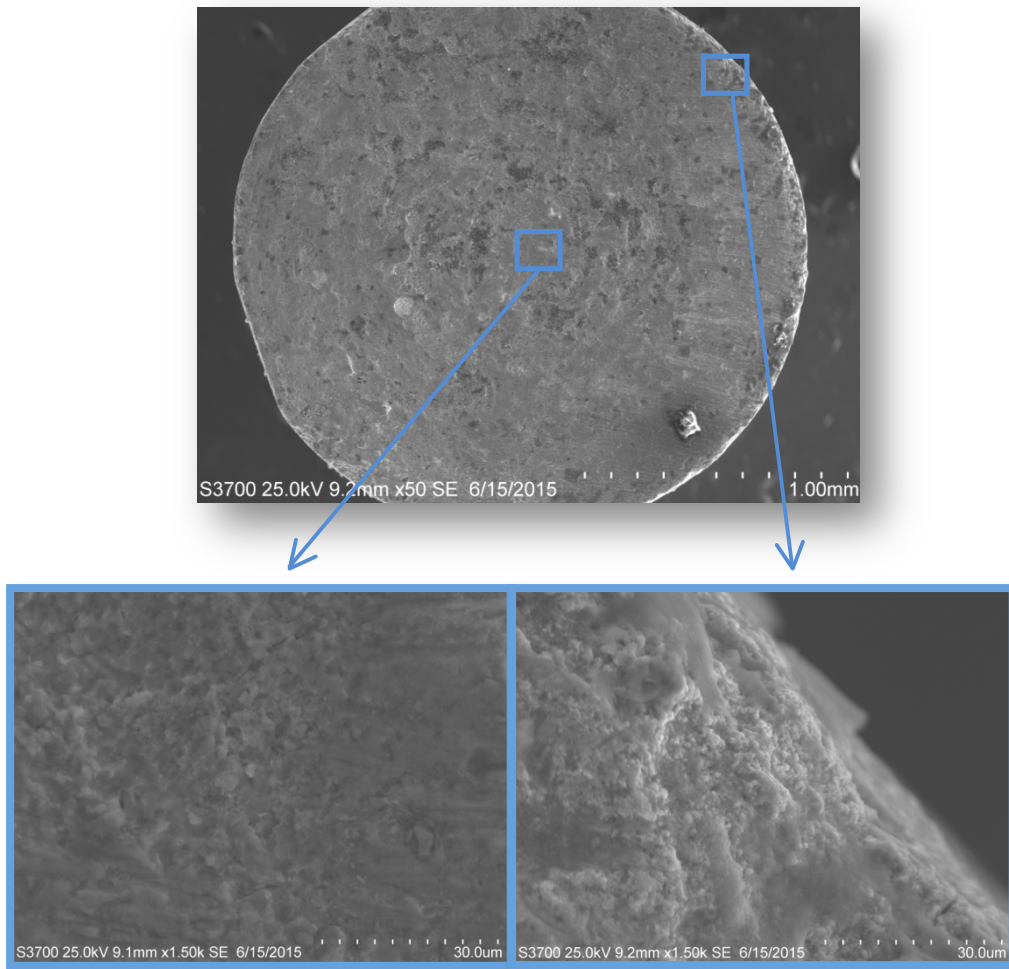


Figure 12. SEM micrograph of the sample YBCO-3 sintered at 850°C and 2 seconds of holding time in the second stage.

4.3.3 YBCO-5



*Figure 13. SEM micrograph of the sample YBCO-5 sintered at 750°C and 2 seconds of holding time in the second stage.*

4.3.4 YBCO-6

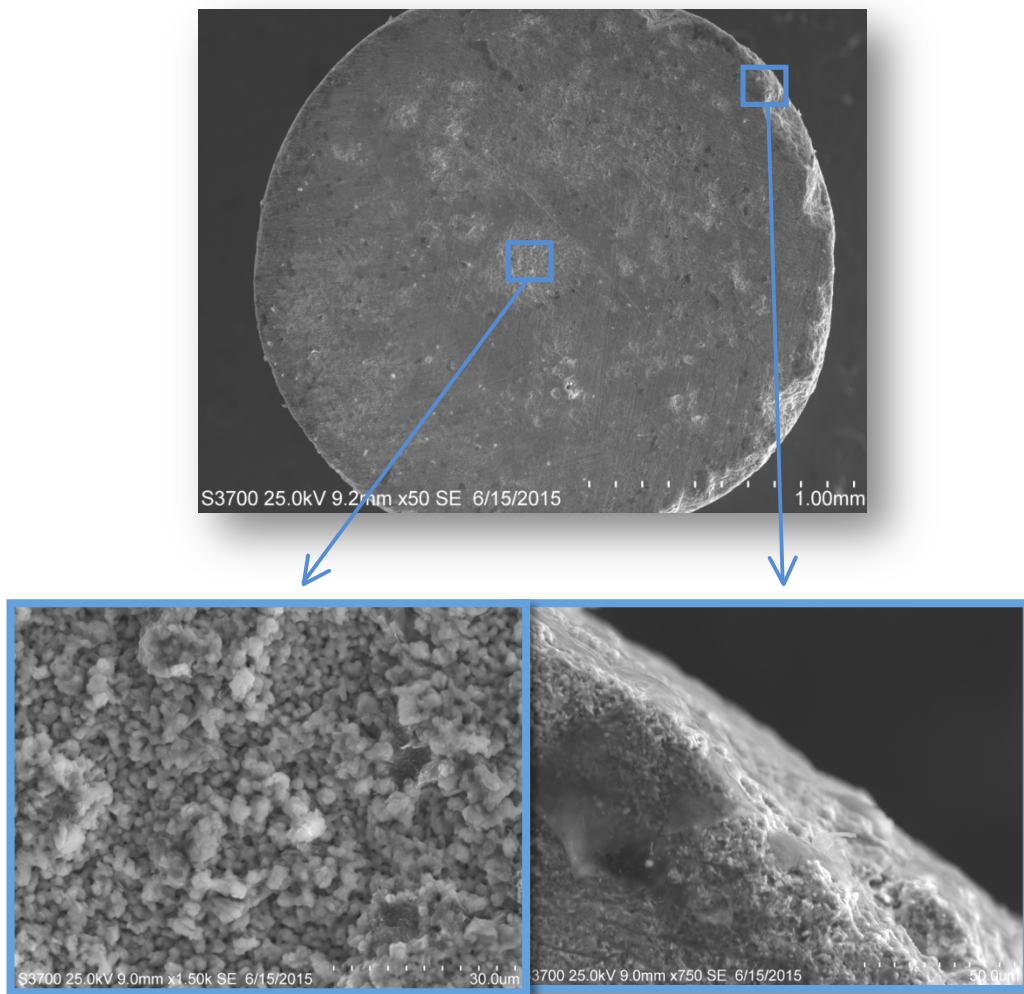


*Figure 14. SEM micrograph of the sample YBCO-6 sintered at 900°C and 2 seconds of holding time in the second stage.*

After the SEM, it was performed the EDX for the surface of each sample. In the following table it can be observed the element content determined by X-ray. These values are only going to be used for observation, as an estimation of the whole elements content is not possible due to the fact that the x-ray is only carried out in a certain area of the surface. As it can be observed, the content of C is high in all the cases, due to the reaction of YBCO with the punch and die, made of graphite.

Sample	C	O	Cu	Y	Ba	Total
<b>YBCO-Test-1</b>	27.02	24.74	5.11	0.00	43.13	100.00
<b>YBCO-3</b>	21.50	27.20	18.11	7.25	25.93	100.00
<b>YBCO-5</b>	43.59	17.43	10.24	5.30	23.44	100.00
<b>YBCO-6</b>	24.59	22.19	13.56	6.75	32.91	100.00

*Table 5. Value of the elements content from the EDX analysis.*

## 5. CONCLUSION

Based on the electrical sintering experiment using the Gleeble 3800 machine provided by the Imperial College in London, there are four powder materials that have been tested with the objective of obtaining the value range of the optimum forming parameters to achieve a high quality dense sample.

As shown in previous section, all the samples presented that have been tested in the experiment carried out could be performed by the technique of Micro-FAST, indicating the powder material of the superconductor YBCO can be sintered at a relative low sintering temperature.

It has been explained in this project that the most important parameters to take into account in the Micro-FAST are the sintering temperature, the pressure, the holding time and the heating rate, which can give the product the desired quality. Based on our experiment, the reduction of the holding time on the second stage of the sintering process makes our sample obtain a lower relative density, especially when the temperature is higher than 750°C. This can be attributed to the short time the temperature is acting on the powder, which can result not enough to perform a good sintering process. This fact can be observed on the micrograph of the SEM, where it can be seen how the microstructure for the case of the samples with higher relative density is more homogeneous than for the other. For example, in the sample YBCO-3, the surface is completely amorphous and rough as the relative density is the lowest.

The pressure applied for the samples are 125MPa for the sample Test-1, as the holding time is of 30s; and 180MPa for the rest of the sample. This increase of pressure is what made possible the sintering process to be carried out, as the temperature could not be transmitted to the samples using a lower pressure. For the case of sample YBCO-3 a first attempt was performed with the pressure of 125MPa and after realizing the fact mentioned before, this pressure was increased. This could be the reason why the sample has not obtained good results speaking of relative density and microstructure.

The sintering temperature distribution was uniform for all the sintered samples, attributed to the symmetric design of the die-set; and the gap between both punches and the die, which is formed after the powders were introduced, disappears after the sintering process. The gap showed a reduction during the heating stage and it is during the holding time period, when the temperature is maintained, when it completely disappears.

It can be concluded that the whole densification process of the superconductor powders of YBCO by Micro-FAST can be performed in a short sintering time. Due to the continuous process of densification, which can involve a plastic

## CHAPTER 5. CONCLUSION

deformation, the grains in the contact areas within two particles can be welded in few seconds, which lead to a fast sintering process.

It can be also found the formation of new grains and the grain refinement can occur when this fast grain-joining process occur, making disappear the interface within two particles. It has to be mention that this is a different sintering process compare to the convectional powder sintering previous processes so many experiments must be carried out until it can be obtained a full understanding of the process and the key parameters for good quality and dense products.

## 6. PROBLEMS TO BE SOLVED

For future experiments performed with this material, several considerations must be taken into account:

- Analysis of the repeatability in the Micro-FAST using these superconductor powders. It has been noticed in previous experiment carried out by the group that, for some other materials the density of the sintered samples was not equal after using the same sintering parameters and raw material.
- Carry out the experiment using another die-set material. Graphite results one of the best material to use for the fabrication of the dies and punches, as its melting point is high enough to undertake the entire sintering process without melting. However, it has been found in different reports, and demonstrate with our sample that a reaction with YBCO is found, making the samples have worse quality.
- Find a proper XRD machine to analyse micro size samples. The content of oxygen is one of the main interest factors to be analysed in these samples and it can be estimated with the XRD, which can give information of the value of the *c*-lattice parameter. With this value it can be observed if the dense body can act as a superconductor or not at a certain temperature and also the time needed for the annealing process in case the sample show a low content of oxygen.
- Increase of the density. Even the density can be improved after an annealing process; it can be found better parameter for the Micro-FAST in order to obtain higher value of the relative density.
- Analyse the superconducting properties. This project is more focus on the study of the mechanical and chemical consideration and features of the samples obtained, however after finding the time require for the annealing process, the superconductivity can be studied easily as this material can act as a superconductor with liquid nitrogen as a cooler.
- Perform the Micro-FAST in oxygen atmosphere. The influence of the atmosphere in this material is a very important factor to take into consideration. It would be also interesting to perform these experiments in a oxygen atmosphere.
- The use of only one machine for annealing and sintering. It would be a very important improvement if the same machine can perform both processes.

**7. REFERENCES**

- [1] A. E. Rokhvarger and L. A. Chigirinsky. *Journal of Electronic Packaging* 26. Vol. 126 (2004)
- [2] Silsbee, F. B. and J. Wash. *Acad. Sci.* 6, 597 (1916)
- [3] D. R. Lundy, L. J. Swartzendruber and L. H. Bennett. *A brief review of recent superconductivity research at NIST. Journal of research of the NIST* Vol. 94, n. 3 (1989).
- [4] Maxwell, E. *Phys. Rev.* 78, 477 (1950)
- [5] Reynolds, C. A., Serin, B., Wright, W. H. and Nesbitt, L. B. *Phys. Rev.* 78, 487 (1950)
- [6] Bednorz, J. G. and Müller, K. A. *Phys. B-Condensed Matter* 64, 189 (1986)
- [7] Müller, K. A. and Bednorz, J. G. *Science* 237, 1133 (1987)
- [8] Tagaki, H., Uchida, S., Kitazawa, K. and Tanak, T. *Japan. J. Appl. Phys.* 26, L123 (1987)
- [9] Wu, M. K, Ashburn, J. R., Torng, C. J., Hor, P. H., Meng, R. L., Huang, Z. L., Wang, Y. Q. and Chu, C. W. *Phys. Rev. Lett.* 58, 908 (1987)
- [10] Pathak, L. C. and Mushra, S. K. *A review on the synthesis of Y-Ba-Cu-oxide powder. Supercond. Sci. Technol.* 18 67-89 (2005)
- [11] Ruckenstein, E., Narain, S. and Wu, N. L. *J. Japan. Soc. Powder Metall.* 37 131-3 (1989)
- [12] Sudareva, S. V., Romanov, E. P., Krinitsina, T. P., Deryagina, I. L., Khelebova, N. E. and Ikyukhin-Yu, V. *sverhprovodimost: Fiz, Khim. Tekh.* 7 1049-57 (1994).
- [13] Saxena, A. K. Book: *High-Temperature Superconductors*. 2010, XIV, 224p.
- [14] Md. AtikurRahman, Md. ZahidurRahaman, Md. NurushSamsuddoha. *American Journal of Physics and Applications*. Vol. 3, No. 2, 2015, pp. 39-56
- [15] S. J. Rothman, J. L. Routbort, and U. Welp. *Phys. Review B* Vol. 44, No 5 (1991)
- [16] J. D. Jorgensen, M. A. Beno, D. G. Hinks, L. Soderholm, K. J. Volin, R. L. Hitterman, J. D. Grace and Ivan K. Schuller. *Phys. Rev. B* Vol. 36, No 7 (1987)
- [17] P. Benzia, E. Bottizzoa, N. Rizzi. *J. of Crystal Growth* 269 (2004) 625–629
- [18] K. Marken. High temperature superconductors for energy applications. 27 (2012) 3-33
- [19] K. Marken. In *High Temperature Superconductor for Energy Applications* pg14-15 (2012)
- [20] A. Koblischka-Veneva, N. Sakai, S. Tajima and M. Murakami. *Handbook of Superconducting Materials*. (Vol. I) 893-947 (2003)
- [21] A. Koblischka-Veneva, N. Sakai, S. Tajima and M. Murakami. *Handbook of Superconducting Materials*. (Vol. I) 893-947 (2003)
- [22] A. Schilling, A. Bernascon, H. R. Ott and F. Hulliger *Physica C* 169 237 (1990).
- [23] A. Junod, D. Eckert, T. Graf, E. Kaldis, E. Karpinski, S. Rusiecki, D. Sanchez, G. Triscone and J. Muller *Physica C* 168 47 (1990)

## CHAPTER 7. REFERENCES

- [24] T. Laegreid, K. Fossheim, E. Sandvold and S. Julsurd *Nature* 330 637 (1987)
- [25] M. D. N. Reguerio and D. Castello. *Int. J. Mod. Phys. B* 5 (2003)
- [26] A. Koblischka-Veneva, N. Sakai, S. Tajima and M. Murakami. *Handbook of Superconducting Materials*. (Vol. I) 893-947 (2003)
- [27] K. Higashida and N. Narita Sendai (Springer: Tokyo) p 805 (1991)
- [28] A. M. Luiz. *Applications of High-Tc Superconductivity*. Intech (2011)
- [29] B. D. Josephson. *Physics Letters*. Vol. 1, No. 7 (1962)
- [30] J. Clarke, *Scientific American* 271, 46 (1994)
- [31] B. A. Willemsen, *IEEE Trans. Appl. Supercond.* 11 (2001) 60
- [32] M. Hidaka, T. Satoh, N. Ando, M. Kimishima, M. Takayama, S. Tahara, *Phys. C* 357-360 (2001)
- [33] A. Yu. Kidiyarova-Shevchenko, D. E. Kirichenko, Z. Ivanov, F. Komissinsky, E. A. Stepancov, M. Khapaev and T. Claeson, *Physica C* 326-327 (1999) 83
- [34] D. A. Cardwell, and D. S. Ginley. *Handbook of Superconducting Materials*. Volume I (2003)
- [35] L. C. Pathak and S. K. Mishra. *Supercond. Sci. Technol.* 18 (2005) 67–89
- [36] L.C. Pathaka, S.K. Mishra, D. Bhattacharya , K.L. Chopra. *Materials Science and Engineering B* 110 (2004) 119-131
- [37] K. Lu. *International Materials Reviews* (2008) VOL 53 NO 1 21
- [38] S. Rahmat. *International Conference on Advance Science and Contemporary Engineering* (2012) VOL 50 369-380
- [39] Eugene A. Olevsky. *Materials Science and Engineering*, R23 (1998) 41–100
- [40] L. C. De Jonghe and M. N. Rahaman. *Handbook of Advance Ceramics* (2003) chapter 4.
- [41] R. A. Terpstra, P. P. A. C. Pex and A. H. Vries. *Ceramic Processing* (1995).
- [42] N. McN. Alford, T. W. Button and J. D. Birchall *Supercond. Sci. Technol.* 3 1 (1990).
- [43] Masato Murakami and René Flükiger. *Handbook of Superconducting Materials*. Institute of Physics Publishing Bristol and Philadelphia (2003) 245-249.
- [44] N. McN. Alford, J. D. Birchall, W. J Clegg, M. A. Harmer, K. Kendall and D. H. Jones *J. Mater. Sci.* 23 761 (1988).
- [45] *Handbook*
- [46] Terpstra R A, Pex P P A C and de Vries A H (1995) *Ceramic Processing* (London: Chapman and Hall)
- [47] K. Lu. *International Materials Reviews* (2008) VOL 53 NO 1 21
- [48] Y. Kim, K. H. Lee, T.-H. Sung, S.-C. Han, Y.-H. Han, N.-H. Jeong, and K. No. *J. Elect. Mater.* 36 (2007) No. 10
- [49] L. C. Pathak, S. K. Mishra, S. K Das, D. Bhattacharya, K. L. Chopra. *Physica C* 351 (2001) 295-300

- [50] L. C. Pathak, S. K. Mishra, D. Bhattacharya, K. L. Chopra. *Materials Science and Engineering B* 110 (2004) 119–131
- [51] G.C. Kuczynski, *J. Appl. Phys.* 21 (1990) 632.
- [52] L.C. Pathak, S.K. Mishra, D. Bhattacharya, K.L. Chopra, *J. Mater. Res.* 14 (1999) 4148.
- [53] Weule, H.; Huntrup, V.; Thies, U.; Schunemann, M.; Bierhals, R.: *Wirtschaftliche Potentiale der Miniaturisierung. wtWerkstattstechnik* 89 (1999) 11/12, 481-484
- [54] Westkamper, E.: *Miniaturisierung und Mikrosystemtechnik. wtWerkstattstechnik* 90 (2000) 469
- [55] Yi Qin, A. Brockett, Y. Ma, A. Razali, J. Zhao, C. Harrison, W. Pan, X. Dai, D. Loziak. *Int. J. Adv. Manuf. Technol.* 47 (2010) 812-837
- [56] M. Geigerl, M. Kleine, R. Eckstein, N. Tieslerl, U. Engel. *Microforming*
- [57] F. Vollertsen: *Production Engineering - Research and Development* 2/4 (2008) 377-383.
- [58] K. F. Zhang, L. Kun. *Journ. of Mater. Process. Technol.* 209 (2009) 4949-4953
- [59] F. Vollertse, H. Schulze Niehoff, Z. Hu. *Int. Jour. Of Mach. Tools & Manuf.* 46 (2006) 1172-79
- [60] S. Hong, H. Hoffmann, *Study of scaling effect on mechanical properties for mill-forming of sheet metal— tensile test of a very thin sheet.* F. Vollertsen, F. Hollmann (Eds.), *Process Scaling*, BIAS Bremen, Verlag, 2003, pp. 145–151.
- [61] E. Egerer, U. Engel, *Process characterization and material flow in microforming at elevated temperatures.* *Journal of Manufacturing Processes* 5 (1) (2004).
- [62] J. H. Durrell. *Critical Current Anisotropy in High Temperature Superconductors* (2001)
- [63] M. H. Zheng, L. Xiao, H. T. Ren, Y. L. Jiao, Y. X. Chen. *Physica C* 386 (2003) 258-261
- [64] Paola Benzi, Elena Bottizzo, Nicoletta Rizzi. *J. of Cryst. Growth* 269 (2004) 625-629
- [65] M. Karppinen, L. Niinistö, *Supercond. Sci. Technol.* 4 (1991) 334.
- [66] R. Chavdarova, T. Nedeltcheva, L. Vladimirova, *Anal. Chim. Acta* 353 (1997) 325
- [67] T. Nedeltcheva, P. Simeonova, V. Lovchinov. *Analytica Chimica Acta* 312 (1995) 227-229
- [68] I.S. Shaplygin, I.A. Konovalova, E.A. Tishchenko, V.B. Lazarev, *Russ. J. Inorg. Chem.* 33 (1988) 1098.
- [69] T. Nedeltcheva, L. Costadinova, P. Simeonova, V. Lovchinov. *Analytica Chimica Acta* 336 (1996) 223-226
- [70] Zon Mori, Toshiya Doi, and Yoshinori Hakuraku. *J. of Appl. Phys.* 107, 023903 (2010)
- [71] Akihiko Yamaji, Sayaka Maeno, Mirei Tomizawa, Masahiro Arai, Tadaharu Adachi. *Physica C* 335 (2000) 264–267
-

## CHAPTER 7. REFERENCES

- [72] Vazquez-Navarro, M. D., A. Kursumovic and J. E. Evetts. *Boletin De La Sociedad Espanola De Ceramica Y Vidrio* 39(3) (2000) 213-216
- [73] L. C. Pathak, S. K. Mishra, P. G. Mukunda, M. M. Godkhindi, D. Bhattacharya, K. L. Chopra. *J. of Materials Sci.* 29 (1994) 5455-5461
- [74] F. Vollertsen, H. Schulze Niechoff, Z. Hu. *Int. Journ. of Mach. Tools and Manuf.* 46 (2006) 1172-1179
- [75] Yi Qin. *Journal of Mater. Proc. Technol.* 177 (2006) 8-18
- [76] K. Huang, Y. Yang, Y. Qin, G. Yang and D. Yin. *Scripta Materialia* 99 (2015) 85-88
- [77] D. Lu, Y. Yang, Y. Qin, G. Yang, J. *Microelectromech. Systems*. Vol. 22, No. 3 (2013) 708 -715.
- [78] K. Huang, Y. Yang, Y. Qin, G. Yang, *Mater. Manuf. Processes* 28 (2013) 183.
- [79] K. Huang, Y. Yang, Y. Qin, G. Yang, *Int. J. Adv. Manuf. Tech.* 69 (2013) 2651
- [80] M. Zadra, F. Casari, L. Girardini and A. Molinari. *Powder. Metall.* Vol. 50, No. 1 (2007) 40-45
- [81] Specific manual of Gleebe 3800
- [82] *High-Temperature Superconducting Materials Science and Engineering*. Douglu Shi. Elsevier (1995)
- [83] *Handbook of Superconducting Materials. Vol. I Superconductivity, Materials and Processes* (2003)
- [84] R. Gladyshevskii and P. Galez. *Crystal structures of high-Tc superconducting cuprates Handbook of Superconductivity* Ch. 8 (2000)